Evaluation of precipitation measurement methods using data from precision lysimeter network

Tobias Schnepper[1, 2, 3], Jannis Groh[1, 4, 5], Horst H. Gerke[4], Barbara Reichert[2], Thomas Pütz[1]

[1]Institute of Bio- and Geoscience IBG-3: Agrosphere, Forschungszentrum Jülich GmbH, Jülich, 52428, Germany
[2]Institute for Geosciences, University of Bonn, Nussallee 8, Bonn, 53113, Germany
[3]GFZ German Research Centre for Geosciences, Telegrafenberg, Potsdam, 14473, Germany
[4]Leibniz Centre for Agricultural Landscape Research (ZALF), Research Area 1 "Landscape Functioning", Working Group "Hydropedology", Eberswalder Straße 84, Müncheberg, 15374, Germany
[5]Institute of Crop Science and Resource Conservation - Soil Science and Soil Ecology, University of Bonn, Nussallee 13, Bonn, 53113, Germany

Correspondence to: Tobias Schnepper (tobias.schnepper@gfz-potsdam.de)

Abstract. Accurate precipitation data are essential for assessing the water balance of ecosystems. Methods for point precipitation determination are influenced by wind, precipitation type and intensity and/or technical issues. High-precision weighable lysimeters provide precipitation measurements at ground level that are less affected by wind disturbances and are assumed to be relatively close to "true" precipitation. The problem in previous studies was that the biases on precipitation data introduced by different precipitation measurement methods were not comprehensively compared and quantified with those obtained by lysimeters under different climatic conditions.

The aim was to quantify measurement errors of standard precipitation gauges as compared to the lysimeter reference and to analyse the effect of precipitation correction algorithms on the gauge data quality. Both correction methods rely on empirical constants to account for known external influences on the measurements, following a generic and a site-specific approach. Reference precipitation data were obtained from high-precision weighable lysimeters of the TERrestial Environmental Observatories (TERENO)-SOILCan lysimeter network. Gauge types included tipping bucket gauges (TBs), weighable gauges (WGs), acoustical sensors (ASs), and optical laser disdrometers (LDs). The data were collected from 2015–2018 at three sites in Germany and compared with a temporal resolution of 1 hour for precipitation above a threshold of 0.1 mm h^{-1}.

The results show that all investigated measurement methods underestimated the precipitation amounts relative to the lysimeter references for long-term precipitation totals with catch ratios (CRs) between 33–92 %. Data from ASs had overall biases of -0.25 to -0.07 mm h^{-1}, while data from WGs and LDs showed the lowest measuring biases (-0.14 to -0.06 mm h^{-1} and -0.01 to -0.02 mm h^{-1}). Two TBs showed systematic deviations with biases of -0.69 to -0.61 mm h^{-1}, while other TBs were in the previously reported range with biases of -0.2 mm h^{-1}. The site-specific and generic correction schemes reduced the hourly measuring bias by 0.13 and 0.08 mm h^{-1} for the TBs and by 0.09 and 0.07 mm h^{-1} for the WGs and increased long-term CRs by 14 and 9 % and by 10 and 11 %, respectively.

It could be shown that the lysimeter reference operated with minor uncertainties in long-term measurements under different climatic conditions. The results indicate that even with well-maintained and professionally operated stations, considerable precipitation measurement errors can occur, which generally lead to a loss of recorded precipitation amounts. Data from standard precipitation gauges therefore still represent potentially significant uncertainty factors. The results suggest that the application of relatively simple correction schemes, manual or automated data quality checks, instrument calibrations and/or adequate choice of observation periods can help improve the data quality of gauge-based measurements for water balance calculations, ecosystem modelling, water management, assessment of agricultural irrigation needs or radar-based precipitation analyses.

40 **1 Introduction**

The terrestrial part of the hydrological cycle begins typically with events of precipitation or non-rainfall water. Exact precipitation data are essential to determine the ecosystem water balance within the soil-plant-atmosphere continuum (Porporato and Rodriguez-Iturbe, 2002). To obtain information on local precipitation amounts, point precipitation measurements are carried out using catching and non-catching precipitation gauges (WMO, 2018). At regional and global

45 scales, precipitation measurement networks connecting a variety of rain gauges provide data to calibrate radar precipitation estimates, climate models and hydrological cycles (Michaelides et al., 2009; Tapiador et al., 2017). Therefore, point precipitation measurements have been intensively studied and several methods for determining precipitation have been developed (WMO, 2018). Depending on the design and functionality of the measuring devices, different errors were identified that affect the precipitation measurements (e.g., Fuchs et al., 2001; Sevruk, 1987; Sevruk and Chvíla, 2005) and therefore also

50 hydrological models (Bárdossy et al., 2022). Especially the influence of wind has been shown to negatively affect point precipitation measurements (Chvíla et al., 2005; Duchon and Essenberg, 2001; Pollock et al., 2018; Sevruk et al., 1989). The effect depends on wind speed, shielding, the shape of the precipitation gauge and the size, phase and fall velocity of the hydrometeors (Kochendorfer et al., 2017b; Sevruk and Nespor, 1994; Wolff et al., 2015). The use of wind shields (Alter, 1937; Nipher, 1878) can reduce the measuring bias, depending on the shields' design (Kochendorfer et al., 2017a; Watson et al.,

55 2008; Yang et al., 1999a). In order to quantify erroneous point precipitation measurements and to minimise the influence of wind, ground-level gauges were developed (Goodison et al., 1998; Lanza and Vuerich, 2009; Sevruk and Hamon, 1984). The data obtained from these gauges were used as a reference for comprehensive comparisons of precipitation gauges for solid (Goodison et al., 1998) and liquid precipitation (Lanza and Vuerich, 2009). The comparative studies led to the development of correction methods that are applied during the post-processing of the data (Førland et al., 1996; Richter, 1995; Sevruk,

60 1982).

Weighable lysimeters were recognised in the 1960s as reference system for precipitation gauge comparisons with measurements at the soil surface (McGuiness, 1966; Morgan and Lourence, 1969). Lysimeters were originally developed to determine and quantify soil and plant related processes such as drainage, evapotranspiration, ion exchange, root development and solute transport (Goss and Ehlers, 2009; Hertel and Unold, 2013). A direct determination of precipitation with weighable

65 lysimeters has been limited in the past by relative coarse temporal resolution (> 10 minutes to daily) and precision. Within the TERrestial Environmental Observatories (TERENO)-SOILCan lysimeter network, high-precision weighable lysimeters are used that are operating with a high temporal resolution (< 1 minute; Pütz et al., 2016). These lysimeters have been successfully used for monitoring precipitation, dew and hoar frost for soil-ecosystems (Gebler et al., 2015; Groh et al., 2018b; Schrader et al., 2013) with a greater resolution and precision than most common gauges (Xiao et al., 2009b).

70 To assure data quality and reliable accuracy of lysimeter-derived precipitation measurements, Marek et al. (2014) stated, that the pre- and post-processing of lysimeter data were highly important. Time series of lysimeter mass changes are oscillating and temporally autocorrelated (Herbrich and Gerke, 2016). Noise filtering algorithms have therefore been developed since the 2010s to reduce the influence of ambient noise on the data (Hannes et al., 2015; Nolz et al., 2013; Peters et al., 2014; Ross et al., 2020; Vaughan and Ayars, 2009) . The "adaptive window and threshold filter" (AWAT; Peters et al., 2014) executes two

75 steps to process the data towards a correction of time-variable noise levels (Peters et al., 2017; Peters et al., 2016). This filter solved the problem of underestimating the lysimeter mass change signals at the turning point from precipitation to evapotranspiration or vice versa; it yields an almost unbiased representation of the real signal which is especially important for the quantification of smaller flux rates such as those caused for instance by dew formation (Groh et al., 2018b; Xiao et al., 2009a).

80 The increased lysimeter data quality (i.e. precision and temporal resolution) has already led to a number of studies that compared lysimeter measurements with those of other precipitation gauges (Gebler et al., 2015; Haselow et al., 2019; Hoffmann et al., 2016; Kohfahl and Saaltink, 2020; Schrader et al., 2013). Gebler et al. (2015) found a 16 % underestimation

of tipping bucket gauge (TB) measured precipitation totals compared to lysimeter data for one year, with 17 % of the difference due to rime and dew and 5.5 % due to fog and drizzle. Snow formation also contributed to the deviations, although the authors

85   identified problems with snow bridges and snow drift interfering with the lysimeter measurements (Gebler et al., 2015). Haselow et al. (2019) compared precipitation measured with a piezoelectric precipitation sensor, a standard TB and a weighable lysimeter. They found an underestimation by the TB and an overestimation by the piezoelectric sensor compared to the lysimeter measurements. Kohfahl and Saaltink (2020) compared precipitation measurements of a precision lysimeter with two TBs and one weighable rain gauge. The authors found good agreement between the measured data from one TB rain gauge,

90   the weighable rain gauge and the lysimeter, while recommending correction of the data from the other TB which underestimates precipitation intensities compared to the lysimeter reference.

Within the framework of the TERENO-SOILCan lysimeter network, numerous point precipitation measurement gauges are under operation, producing data with 10-min resolution (Pütz et al., 2016). Up to four different rain gauges are installed in the immediate vicinity of the lysimeter stations and their data can be publicly accessed through the TERENO data platform

95   (https://ddp.tereno.net/ddp/; for details see "Data availability"; Kunkel et al., 2013). The lysimeter data available within the network is comprehensively processed and tested and has been used for a variety of studies in the field of soil and plant sciences (Groh et al., 2019; Groh et al., 2020a).

For this study, we hypothesise that values derived from hourly precipitation data of high-precision weighable lysimeters can function as reference for a comparison of multiple precipitation measuring methods. To test this, data from multiple lysimeters

100   installed at respective test sites are graphically compared via scatter plots, a correlation coefficient, and deviations to the arithmetic mean. Furthermore, we hypothesise that if the precipitation measurements of the considered methods are affected by external influences, then the gauge measurements should be on average lower than the ones determined by the lysimeter references for all devices of the same gauge model at all sites. To test this, we compare hourly precipitation amounts as well as long-term precipitation totals determined by these measuring methods with reference data derived from high-precision

105   weighable lysimeter data via scatter plots and appropriate statistics for all three sites, also considering measuring uncertainties. The final hypothesis is that the use of precipitation correction methods that consider the influence of wind and other typical sources of error on the instruments will reduce the bias between reference and measurements and increase the data quality close to zero. Therefore, two correction methods are applied on the tipping bucket and weighable gauge data during post-processing, and the influence on the bias and overall deviations from the references is studied by comparing the resulting data

110   with the reference lysimeter-based precipitation.

To conduct this study, high-quality long-term data of four years (2015–2018) from 15 lysimeters, four different types of precipitation measuring methods (11 devices) of three research sites and local weather data with a resolution of 1 hour are available.

2 Material and methods

115   **2.1 Research sites**

The data were collected at research sites near Dedelow (DD), Rollesbroich (RO) and Selhausen (SE) in Germany, which are all part of the TERENO-SOILCan network (Fig. 1; Pütz et al., 2016). The TERENO-SOILCan lysimeter network itself belongs to the TERENO project (Zacharias et al., 2011) and comprises twelve different lysimeter research sites in Germany (Pütz et al., 2016). The network purpose is to enable insights into effects of climate change on arable and grassland ecosystems,

120   including water balance components. To achieve this, a modified space-for-time concept was used, where lysimeters filled with four different soils have been transferred within the TERENO observatories to simulate a time-induced change of climate through a space-induced change of climate for studying effects on crop productivity and soil water and plant nutrient balances (Groh et al., 2020a; Groh et al., 2020b; Pütz et al., 2016). The lysimeters have been used to estimate precipitation and actual

evapotranspiration (Gebler et al., 2015; Groh et al., 2019; Schrader et al., 2013) as well as non-rainfall water that arises from

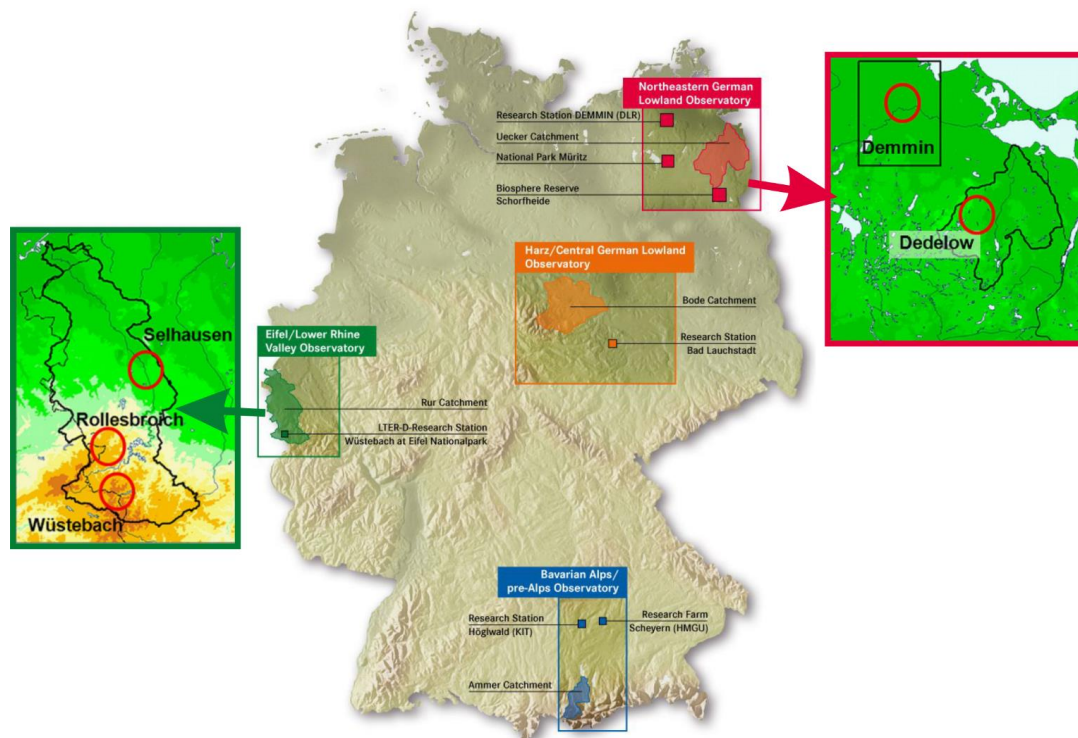125 the formation of dew, hoar frost and rime (Groh et al., 2018b; Meissner et al., 2007).

Figure 1: The TERrestial Environmental Observatories (TERENO)-SOILCan network (adapted from Pütz et al., 2016). The data for this study was collected at sites near Dedelow (Northeastern German Lowland Observatory), Rollesbroich and Selhausen (both Eifel/Lower Rhine Valley Observatory).

130 RO, as part of the Eifel/Lower Rhine Valley Observatory, is situated in the northern part of the Eifel, which is a low mountain range in Western Germany (Bogena et al., 2018). The area is widely open and comprises extensively used grassland. The elevation of the site (511 m above sea level) leads to a mean annual precipitation of 1063 mm a^{-1} (DWD, 2021a; 50°38'; 06°12') and a mean annual temperature of 7.7 °C (DWD, 2021b; 50°38', 06°12').

The site in SE is situated in the plain lower Rhine valley and is surrounded by extensively used arable land (Bogena et al.,

135 2018). It is located in the temperate maritime climate zone with a mean annual temperature of 9.8°C (DWD, 2021b; 50°56', 06°34') and a mean annual precipitation of 723 mm a^{-1} (DWD, 2021a; 51°56', 06°34').

The test site near DD is in the Northeastern German Lowland Observatory of TERENO (Heinrich et al., 2018), approximately 100 km north of the city of Berlin. At the site, a hummocky ground moraine landscape is characterized by lakes and arable land (Heinrich et al., 2018). The lysimeter station is surrounded by arable land. A mean annual temperature of 7.9 °C (DWD,

140 2021b; 53°19', 13°56') and a mean annual precipitation of 504 mm a^{-1} (DWD, 2021a; 53°17', 13°56') have been determined for the area around the test site in Dedelow.

2.2 Equipment and data collection

2.1.1 TERENO-SOILCan Lysimeter

The weighable high-precision lysimeters used within the TERENO-SOILCan network are comparable to the "Scientific Field

145 Lysimeter" described by Unold and Fank (2008). The lysimeters are equipped with soil moisture probes, soil water sampling

Hydrology and
Earth System
Sciences
Open Access
Discussions

EGU

devices, tensiometer, a precision weighable system, a thermal flux sensor and silicon carbide porous suction cups (Pütz et al., 2016). Every lysimeter has a surface of 1 m² and a depth of 1.5 m. They are connected to a central service well which contains the power supply, data loggers, measuring transducers, pumps, seepage water tanks including weighable systems, sampling bottles and a data modem (Pütz et al., 2016). For detailed information about the installed sensors and the lysimeter filling, see

150 Pütz et al. (2016) and Hertel and Unold (2013).

All lysimeters used in this study are of the same type and disposed in lysimeter stations which comprise at least one hexagon of six lysimeters placed around the central service well (Fig. 2 B; Pütz et al., 2016). The weighable systems consist of three load cells (Model 3510, Tedea-Huntleigh, Canoga Parl, CA, USA) with a resolution of 10 g ≅ 0.01 mm precipitation and are mounted at each lysimeters bottom. A gap between lysimeter and the concrete housing is closed with a synthetic resin collar,

155 which is covered with surrounding soil. The small remaining gap between the collar and the lysimeter is closed with silicone foil fixed at the resin collar, but without any direct contact to the lysimeter vessel to prevent any disturbance on the lysimeter weighing. This ensures a smooth suspension and weighing of the lysimeter (Pütz et al., 2016). The lysimeters were intensively maintained at least every week and the incoming data were daily checked for irregularities and anomalies. To ensure a stable environment for the observations, the type of lysimeter filling remains the same during the observation period. The surrounding

160 areas were similarly managed as the lysimeters to prevent an "isle effect", that would have affected the determination of precipitation due to exposed vegetation (Hagenau et al., 2015). On the arable lysimeters the crop rotation was winter wheat, winter barley, winter rye and oat during the observation period (2015–2018). No catch crop between the growing seasons was grown. In general, the agricultural activities were in accordance with common agricultural practice (Pütz et al., 2016). The grass lysimeters were cut three to four times per year.

165 Based on the mass changes of a lysimeter and a seepage water tank, the water fluxes across the soil surface were calculated using the lysimeter water balance (Schrader et al., 2013). The water balance equation for a lysimeter follows:

$$\Delta W = P + NRW - ET_a - D, \tag{1}$$

where ΔW is the change in the lysimeter mass, P the precipitation, NRW non-rainfall water, ET_a the actual evapotranspiration and D the drainage. The amount of precipitation is calculated from any increase in lysimeter mass after correction with water

170 fluxes across the lysimeter bottom. It was assumed that no evaporation or transpiration occurred during the specific time period (Schneider et al., 2021; Schrader et al., 2013; Eq. 2). Any decrease of the lysimeter mass change after the correction with fluxes across the lysimeter bottom can thus be related to evapotranspiration if no precipitation occurred during this time interval (Eq. 3).

$$P_i = \begin{cases} WL_i - WL_{i-1} + WT_i - WT_{i-1} > 0 \\ 0 \; for \; WL_i - WL_{i-1} + WT_i - WT_{i-1} \le 0 \end{cases} \tag{2}$$

175 $$ET_i = \begin{cases} -(WL_i - WL_{i-1} + WT_i - WT_{i-1}) \\ for \; WL_i - WL_{i-1} + WT_i - WT_{i-1} < 0 \; , \\ 0 \; for \; WL_i - WL_{i-1} + WT_i - WT_{i-1} \ge 0 \end{cases} \tag{3}$$

where P_i is the precipitation amount during time interval i (kg), WL is the lysimeter mass in terms of the weight (kg), WT is the seepage tank weight (kg) and ET_i is the evapotranspiration amount during time interval i (kg).
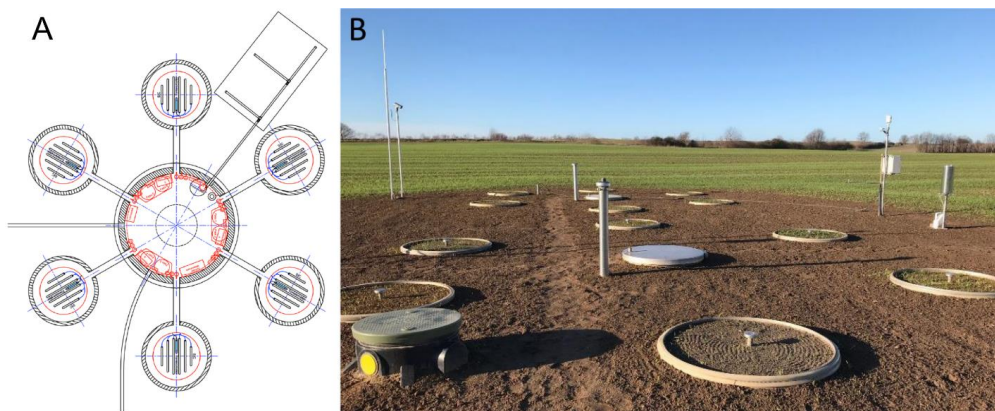
Figure 2: A) Technical drawing of the lysimeter hexagon from birds view (from Pütz et al., 2016, provided by UMS AG, Munich, Germany).
180   B) Two lysimeter hexagons at ZALF's research station in Dedelow (photo by Hannah Kimmich).

2.2.2 Precipitation gauges

Two variants of the same tipping bucket gauge model (TB; "ecoTech Umwelt-Meßsysteme GmbH", Bonn, Germany) are used at the test sites, which differ in the collecting surface of 200 cm² for SE and RO and 400 cm² for DD. The measuring mechanism bases on a funnel with an inlet water pipe which leads the caught precipitation into a tipping bucket, which, when filled with
185   a certain amount of water, tips to either side of the sharp edge pivot. The motion is determined by the weight imbalance caused by the water dripping from above. The device registers the number of tips with a magnet mounted on the bucket, inducing a signal to a reed switch. A second TB in RO and the TB in DD are additionally equipped with a heating module. The resolution of the TBs is 0.1 mm which indicates an equal volume of one of the buckets compartments.

The weighable gauge (WG) used in this study is the model Pluvio² manufactured by Ott Hydromet, Kempten, Germany. It
190   uses load cells to determine the differences in weight in the weighing chamber caused by collected precipitation. The gauge has an orifice with a collecting area of 400 cm², a resolution of 0.01 mm and a minimal cumulative precipitation threshold at 60 min collection time of 0.05 mm h^{-1}. The device outputs real-time and processed data with a time lag of a few minutes. A heating module is installed to prevent solid precipitation from blocking the gauges inlet. It merely heats the collecting ring around the orifice to avoid artificial loss due to evaporation. The model was used as reference gauge in multiple studies
195   (Johannsen et al., 2020; Kochendorfer et al., 2017a; Ryu et al., 2016) and was one of the most widely used WGs according to a survey within the WMO members in 2008 (Wong and Nitu, 2010). On the 2017/07/19, a single Alter wind shield was installed around the gauge in SE. This type of shield consists of loose hanging lamellas, which are mounted on a concentric ring around the gauge (Alter, 1937) and is widely established to prevent wind loss and recommended by several institutes (Dengel et al., 2018).

200   The weather station WXT510 (Vaisala Oyi, Helsinki, Finland) is installed at all sites to measure meteorological standard parameter such as wind speed, wind direction, air temperature, relative humidity, and barometric pressure at 2 m height. The station includes the Vaisala RAINCAP® sensor, an acoustic sensor (AS) with a resolution of 0.01 mm h^{-1} (Salmi and Ikonen, 2005). The AS relies on a piezoelectric detector with a surface of 60 cm², with which the impact of individual raindrops on the surface is measured. Raindrops collide with the surface at their terminal velocity, which is a function of the raindrop diameter.
205   Depending on the terminal velocity and the mass of the raindrop, every collision creates a particular signal, which is proportional to the volume of the drops, and is then converted to an individual voltage by the piezoelectric detector (Winder and Paulson, 2012). The voltage pulses are filtered, amplified, digitized, and analysed. Knowing the voltage signals per unit time and the surface area, rain duration and -intensity can be determined. Each type of precipitation creates a distinguishable signal which enables the detection of liquid and solid precipitation. Since the terminal velocity of snow is low, the AS can only
210   differentiate between rain and hail.

The laser disdrometer (LD; Adolf Thies GmbH & Co KG, Göttingen, Germany) is installed on the sites in RO and SE. The instruments use an infrared light-beam with a wavelength of 780 nm and a cross section of approx. 46 cm². It records the reduction of the transmitted light intensity by particles falling through the light-beam and can therefore derive the particle diameter. The strength and duration of the attenuation initiated by the falling particle allows for an inference of its diameter

215 and velocity, such that the precipitation type, rain and snow, can be distinguished (Bloemink and Lanzinger, 2005; Fehlmann et al., 2020). The LD distinguishes precipitation with a diameter of 0.125 mm and derives the vertical velocity by the measured signal duration (Lanzinger et al., 2006). It offers a low sensitivity threshold with a resolution of 0.001 mm h^{-1}.

Weather data as well as precipitation data from TB, WG and AS are stored on a data logger at DD, RO, and SE (all "envilog Maxi", ecoTech, Bonn, Germany) at 10-minutes intervals (Pütz et al., 2016). Weighing data from the lysimeters are stored in

220 a data logger (1-minute intervals, DT85, Datataker-Thermo Fisher Scientific Australia Pty Ltd., Scoresby, VIC, Australia), whereas the LD´s data is stored on a local memory card.

2.3 Data processing

Lysimeter data, which are available as time series of mass changes in minute resolution, were pre-processed in three steps: i) check of the minutely monitored raw data time series' for plausibility (manually and automatically), ii) application of the

225 AWAT-filter to reduce the impact of noise on the raw data of the lysimeter mass changes (Peters et al., 2017), and iii) summing the minutely to hourly values; note that hours with missing values were marked as not available (NA).

Weather and gauge precipitation data were similarly treated with a plausibility check (manually and automatically) and an aggregation to hourly values. For this, the precipitation measurements present for 10-minutes intervals were summed, while the 10-minutes measurements from the climate stations such as temperature (°C), wind speed (m s^{-1}) and wind direction (°)

230 were averaged over one hour.

To determine whether the gauge data then add up to comparable hourly values and to be able to eliminate potential time lags between all devices, representative precipitation events were analysed by comparing the 10-minutes with the hourly resolution (Appendix A1). Since the lysimeter measurements function as reference for the comparison, they are intended to mark the beginning of an event as well as significant peaks within a precipitation event. The comparison revealed a time lag of ten

235 minutes between lysimeter and gauge data, which is due to time stamps from different data loggers. Another time lag for the WG data was induced by gauge-internal processing. Adjusting the overall gauge data with a 10-minutes inverse time lag and using the raw WG data solved the problem.

2.4 Reference precipitation values and their uncertainties

The derivation of a reference precipitation intensity (P_{ref}; mm h^{-1}) for the comparison of precipitation data is critical for further

240 investigations. It was chosen to compute the mean measured precipitation among the lysimeters for each hourly data point (Eq. 4), when at least half of the lysimeters data were available for that hour. This way it is ensured that the mean is not depending on single measurements and that too many data points are discarded because of missing values. At sites (SE and DD) where only three lysimeters of the same soil-ecosystem are operated, the mean is calculated when at least two lysimeters provide measurements:

245 $$P_{ref} = \begin{cases} \frac{1}{n}\sum_{i=1}^{n} x_i \ for \ n \geq n_{ia}, \\ NA \ for \ n < n_{ia}, \end{cases} \quad (4)$$

where n is the number of lysimeters providing observations during time interval i (-), x_i the precipitation intensity measured by each lysimeter in the given interval i (mm h^{-1}) and n_{ia} is the number of lysimeters with missing data during time interval i (-).

Following WMO (2018), a rain intensity gauge is required to not exceed defined uncertainties while measuring rain

250 precipitation intensities (P_{gauge}). Under field conditions, an uncertainty of 5 mm h^{-1} for $P_{gauge} < 100$ mm h^{-1} should not be

Hydrology and
Earth System
Sciences
Discussions

Open Access

EGU

exceeded. An approach conducted by Vuerich et al. (2009) derives P_{ref} from the mean of four different reference pit gauges. They calculated the uncertainty for the reference values from standard deviations of precipitation measurements from the pit gauges. The authors use the 95 % confidence level (k=2) deducted from two times the standard deviation of the measurements. To adapt the concept, it was decided to proceed as follows: It is assumed that measurements of the same precipitation event

255   conducted by all available lysimeters are normally distributed. Thus, the standard deviation (SD) between measurements of all lysimeters with the same vegetation cover at each site can be calculated for each hour, where data from all lysimeters is available (Eq. 5). After calculating the lysimeter uncertainties (U_{ref}; Eq. 6) each hour is assigned to a category according to its precipitation intensity value, whereby each category comprises a span of 0.1 mm, resulting in 200 categories for P_{ref} of 0 to 20 mm h^{-1}, which was the maximum observed precipitation intensity during the observation period across all sites. All uncertainty

260   values for hours within the respective category are then averaged and the computed mean is attributed back to the respective hours. This assigns an individual uncertainty value to each precipitation intensity interval. The WMO (2018) recommends to add 5 % of P_{ref} to the gauges uncertainties (here lysimeters; U_{fin}; Eq. 7) as an upper limit for uncertainties of rain gauges. The final uncertainties are then plotted and smoothed using the "*geom_smooth*" function (R, Package: ggplot2; Wickham, 2016) with cubic splines using the R software (R Core Team, 2020) to provide an uncertainty range for the gauge comparison via

265   scatter plots.

$$SD = \sqrt{\frac{\sum_{i=1}^{n}(x_i - \bar{x})^2}{n-1}}, \tag{5}$$

$$U_{ref} = P_{ref} \pm 2 * SD, \tag{6}$$

$$U_{fin} = U_{ref} \pm 0.05 * P_{ref}, \tag{7}$$

with n being the number of observations (-), x_i the precipitation intensities measured by each lysimeter during time interval i

270   (mm h^{-1}), $\bar{x}$ the empiric mean of the lysimeter measurements at the site during time interval i (mm h^{-1}), P_{ref} the reference precipitation intensity during time interval i (mm h^{-1}), U_{ref} the uncertainty of the lysimeter reference during time interval i (mm h^{-1}) and U_{fin} the final uncertainty for the gauge comparison for time interval i (mm h^{-1}). To additionally reduce potential uncertainties and achieve more comparable results when comparing the measurement methods with the lysimeter reference, only data is used with P_{ref} and P_{gauge} both being ≥ 0.1 mm h^{-1}, which is the smallest common resolution of all measuring

275   instruments.

2.5 Determination of key parameters

2.5.1 Non-rainfall events

Non-rainfall events (NRE) comprise the formation of dew, hoar frost, and fog. Hourly precipitation data was categorised as NRE, if no rain gauge except the lysimeters or the disdrometer registered precipitation. The disdrometer was excluded because

280   it could detect fog. Often, combined observations on NREs by leaf wetness (for dew and hoar frost) or visibility sensors (fog) and weighable lysimeters are used to identify NREs (Zhang et al., 2019). No such sensors were available for our sites. Therefore, we followed the approach by Groh et al. (2018b), who restricted the occurrence of NRE to the period between sunset and sunrise without any rainfall detected by WG and the hourly NRE intensity to a maximum rate of 0.07 mm h^{-1} according to assumptions on dew formation by Monteith and Unsworth (2013).

285   #### 2.5.2 Precipitation type and intensity classification

The piezoelectric sensor as well as the optical disdrometer could identify the mentioned precipitation types in a sufficient way (Bloemink and Lanzinger, 2005; Fehlmann et al., 2020; Salmi and Ikonen, 2005). Due to an incomplete data situation, an approach was carried out to derive the precipitation type from the air temperature at the sites. For gauge intercomparisons, temperature ranges of +4 to 0 °C (Gebler et al., 2015), +2.5 to -2.5 °C (Kochendorfer et al., 2017b), +2 to 0 °C (Førland et al.,

290 1996) and +2 to -2 °C (Ryu et al., 2016) were chosen for mixed precipitation. Here the later threshold of +2°C and -2°C was used in this study for mixed precipitation (Table 1). Thus, temperatures above 2°C are used to classify liquid precipitation (rain) and temperatures below -2°C classify solid precipitation (snow). The small number of precipitation events classified as "snow" can be explained by the pre-filtering of the lysimeter measurements influenced by snow bridges or ice formation. Due to the small number of "snow" events and the uncertainties involved in quantifying snow and mixed precipitation with

295 lysimeters and precipitation gauges, hours within both categories are excluded from further investigation.

Table 1: Number of hours of three main precipitation types for the years 2015–2018 according to the lysimeter reference. Hours with no precipitation registered by the lysimeters and non-rainfall events are excluded.

Site	Rain	Mixed	Snow
	(h)	(h)	(h)
Rollesbroich	4695	763	21
Selhausen	3949	186	8
Dedelow	2949	260	4

The classification of precipitation intensities was done in accordance to WMO (2018). Here, observations were classified

300 according to the precipitation registered by the lysimeter reference. Hours with $P_{ref} < 2.5$ mm h^{-1} were regarded as "slight", $2.5 \leq P_{ref} < 10$ mm h^{-1} as "moderate" and $10 \leq P_{ref} < 50$ mm h^{-1} indicated "heavy" rainfall (Table 2).

Table 2: Number of hours classified according to the reference precipitation intensity (P_{ref}) for the years 2015–2018. Hours with no precipitation registered by the lysimeters and hours with non-rainfall events are excluded.

Site	Slight precipitation	Moderate precipitation	Heavy precipitation
	($P_{ref} < 2.5$ mm h^{-1})	($2.5 \leq P_{ref} < 10$ mm h^{-1})	($10 \leq P_{ref} < 50$ mm h^{-1})
	(h)	(h)	(h)
Rollesbroich	5179	269	10
Selhausen	3976	155	4
Dedelow	3073	132	4

305 **2.6 Correlation analyses**

The precipitation measurements between the reference values and those obtained from the gauges were compared based on x-y scatter plots (e.g., Haselow et al., 2019; Liu et al., 2013; Yang, 2014). Within a plot, the uncertainty range, the bias (Eq. 8) as well as the standard deviation of the measurement differences (SDD, Eq. 9), the R²-value (Eq. 10), the number of observations (n) and the linear regression line (Eq. 11) are given. To enhance the visualisation, additional plots and statistics

310 for slight precipitation events are provided.

$$Bias = \sum_{i=1}^n (X_i - Y_i)/n \,, \tag{8}$$

$$SDD = \sqrt{\frac{\sum_{i=1}^n (x_i-y)^2}{n-1}} \,, \tag{9}$$

$$R^2 = \frac{\sum (Y_i-\bar{x})^2}{\sum X_i-\bar{x}}^2 \; with \; \bar{x} = \frac{1}{n}\sum_{i=1}^n X_i \,, \tag{10}$$

where n is the number of observations (-), X_i the reference precipitation intensity during time interval i (mm h^{-1}) and Y_i the

315 precipitation intensity determined by the precipitation gauge during time interval i (mm h^{-1}).

The bias is the average difference between the precipitation measured by the gauge and the reference measurement, so positive or negative values indicate that the gauges generally over- or underestimated precipitation, respectively. The SDD quantifies the distribution of the differences and thus the spread of the data points around the 1:1 reference line. The nondimensional coefficient of determination, R², describes how well the linear regression model, displayed in the plot, fits to the data. Due to

320 its derivation, it is also closely related to the extent of the spread of the data but does not consider the spread around the 1:1

Hydrology and
Earth System
Sciences
Open Access
Discussions
EGU

reference line. The regression lines follow the standard linear regression (Eq. 11) performed in R (R Core Team, 2020), using the "*ggplot2*" package (Wickham, 2016).

$$Y_i = \alpha + \beta X_i, \tag{11}$$

where α and β are regression coefficients.

325   While interpreting the bias, SDD, R²-value and regression lines, it must be considered that these statistics and methods base on the assumption of normally distributed data. Since precipitation data does not follow such a distribution, low precipitation intensities occur more often than higher intensities and therefore the residuals are heteroscedastic, the statistics might be not enough to describe the data distribution. Therefore, an additional, visual illustration of the data was required, as presented by the scatter plots.

330   **2.7 Wind error analysis**

To analyse the influence of wind speed at gauge height (v_g) on the gauge's precipitation measurements, the catch ratio (CR; Eq. 12) is used. The CR can be described as a function of wind speed and temperature (Goodison et al., 1998; Yang et al., 1998). CRs of different gauges were calculated with regression analyses on the basis of reference measurements at multiple sites (Chen et al., 2015; Goodison et al., 1998; Sugiura et al., 2006; Yang et al., 2000). The CR of a gauge and reference values

335   can also be described with following equation:

$$CR = \frac{P_{gauge}}{P_{ref}} * 100 . \tag{12}$$

Since the influence of the temperature can be neglected due to the exclusion of mixed and solid precipitation, the primary parameter to consider is the wind speed at gauge height, which can be derived from the measured wind speed at 2 m above ground (Eq. 13; Goodison et al., 1998):

340    $$v_g = [log(\frac{h_g}{z_0}) / (log(\frac{h}{z_0})] * v_h, \tag{13}$$

where v_g is the wind speed at the height of the gauge orifice (m s⁻¹), h_g the height of gauge orifice above ground (m), z_0 the roughness length (0.01 m in winter, 0.03 m in summer), h the height of the wind speed measuring instrument above ground (m) and v_h the wind speed measured by the measuring instrument (m s⁻¹).

2.8 Precipitation data corrections

345   Sevruk (1982) provides a general equation for the correction of precipitation measurements which is adjusted with regard to an improved readability to the notation by Førland et al. (1996; Eq. 14):

$$P_{cor} = k(P_m + P_w + P_e + P_t) , \tag{14}$$

with P_{cor} being the corrected precipitation (mm), k the correction factor for wind (-), P_m the measured precipitation (mm), P_w the wetting loss (mm), P_e the evaporation loss (mm) and P_t the loss by trace precipitation (mm).

350   Few of the correction methods based on Eq. (13) are developed to correct precipitation measurements on an hourly basis, due to the absence or small numbers of automatic gauge types in the last decades. Førland et al. (1996) published the dynamic correction model (DCM) with which Michelson (2004) corrected hourly precipitation data of four different gauge models mainly used in Scandinavian countries. The correction factor for wind loss, k, can thus be adjusted for hourly rain measurements following the DCM (Førland et al., 1996; Michelson, 2004; Eq. 15):

355    $$k = exp \begin{bmatrix} -0.00101 * ln(P_{gauge}) - 0.012177 * vg * ln(P_{gauge}) + \\ 0.034331 * v_g + 0.007697 + c \end{bmatrix}, \tag{15}$$

where c is the gauge constant (mm 12 h⁻¹).

Hydrology and
Earth System
Sciences
Discussions

Open Access

EGU

Michelson (2004) offers empiric constants for wetting loss, evaporation loss as well as the wind induced error for four different gauge models and precipitation types (Table 3-4). The empiric constants apply for 12 h measuring intervals, which can be derived to an hourly basis. Since evaporation does not account for WGs if it is supressed with an oil film (WMO, 2008), only

360 the gauge constant for determining the wind error has to be chosen for the WG. Michelson (2004) states that precipitation gauge designs, that are similar to the WG used here, have a slightly improved gauge constant compared to the Hellmann gauge (0.0 mm 12 h^{-1}), thus a gauge constant of -0.05 mm 12 h^{-1} is chosen for the WG.

To compensate the loss by trace precipitation for the TB, an empiric value provided by Yang et al. (2001) with a loss of 0.1 mm d^{-1} is assumed for days with at least one precipitation event.

365 **Table 3:** Wetting and gauge constants for Eq. (15) provided by Michelson (2004) for multiple gauge types. SMHI: Gauge used by the Swedish Meteorological and Hydrological Institute.

Precipitation phase	Constant	SMHI (mm 12 h^{-1})	Hellmann (mm 12 h^{-1})
Liquid	Gauge	-0.05	0.00
Liquid	Wetting	0.07	0.14

Table 4: Daily evaporation loss constants for Eq. (15) as provided by Michelson (2004) for multiple gauge types. SMHI: Gauge used by the Swedish Meteorological and Hydrological Institute.

Month	Hellmann (mm 12 h^{-1})
January	0.01
February	0.02
March	0.03
April	0.04
May	0.09
June	0.15
July	0.16
August	0.08
September	0.02
October	0.01
November	0.01
December	0.01

370

Richter (1995) developed a correction method especially for German Hellmann-type gauges installed at sites, where no wind speed can be determined. He used factors depending on the shielding of the site and the precipitation type, based on long term precipitation measurements. The derived daily correction amount includes all relevant losses (including wind, evaporation, trace, and wetting). To test the potential of the correction method by Richter (1995) to be applied on hourly precipitation data,

375 a similar approach to the one published by Gebler et al. (2017) is chosen. The authors initially calculated corrections for daily precipitation data according to Richter (1995; Eq. 16 and 17) and then redistributed it to hourly measurements via the ratio of daily measured to daily corrected data. Here it was decided to redistribute the daily corrections via the number of precipitation hours within a day (Eq. 18):

$$P_d^{cor} = P_d + \Delta P_d, \tag{16}$$

380 $$\Delta P_d = b * P_d^{\varepsilon}, \tag{17}$$

$$P_h^{cor} = \frac{P_d^{cor}}{n_{Pevent}} + P_h, \tag{18}$$

where P_d^{cor} is the corrected daily precipitation (mm d^{-1}), P_d the daily precipitation measured by gauge (mm d^{-1}), ΔP_d the amount of daily additional precipitation (mm d^{-1}), b the coefficient for the influence of wind exposition at the measurements

site (-), P_d^ε the empiric coefficient for the precipitation type (-), P_h^{cor} the corrected hourly precipitation (mm h^{-1}), n_{Pevent} the

385 number of hours with P_{ref} > 0.1 mm h^{-1} within a day (-) and P_h the hourly precipitation measured by the gauge (mm h^{-1}).

3 Results

3.1 Uncertainty range of the lysimeters

With increasing P_{ref} values, the measurement uncertainties from the lysimeters decrease at all sites. The uncertainty ranges indicate that between 1 and 2.5 mm h^{-1} the relative measuring differences decrease to values below 5 % (Fig. 3). For P_{ref} > 8

390 mm h^{-1}, the lack of data does not allow to delineate a clear area of uncertainty. In DD, three rain events with precipitation intensities > 11 mm h^{-1} were associated with increased deviations within the lysimeter measurements, which bias the regression line and therefore the predicted uncertainty range at these precipitation intensities (Fig. 3D).
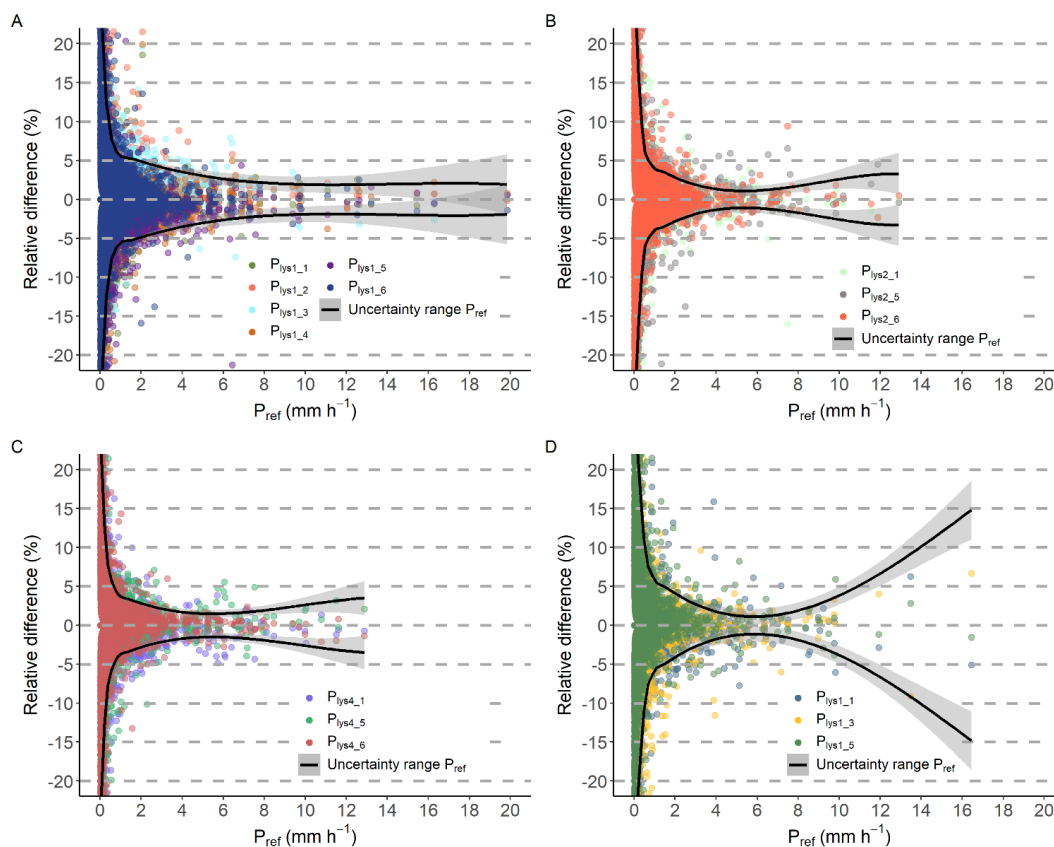

Figure 3: Uncertainty ranges of lysimeter references (P_{ref}), delimited through solid lines, and differences of each lysimeter measurement
395 relative to P_{ref}. A: Rollesbroich lysimeter station, lysimeter with grassland. B: Selhausen lysimeter station, lysimeter with grassland. C: Selhausen lysimeter station, lysimeter with arable land. D: Dedelow lysimeter station, lysimeter with arable land.

3.2 Annual precipitation values

During hours in which all devices at a site were available and at least one gauge (TB, WG or AS) and the lysimeters measured a precipitation intensity of 0.1 mm h^{-1} or higher (Table 5), the TB1 in Rollesbroich (RO) registered 22.9–47.1 % of P_{ref} within
400 each individual year of operation. The TB in Selhausen (SE) caught 20.4–40.7 %, TB2 (RO) 79.2–83.8 % and the TB in Dedelow (DD) 72.8–84.0 %. The WGs caught 82.2–89.0 % (RO) and 89.4–94.5 % (SE), respectively. The AS measured 62.8–78.2 % (RO), 70.0–82.1 % (SE) and 82.6–91.3 % (DD). The LD (RO) measured 85.7–95.3 %, while the LD (SE) measured

73.6–96.1 %. Deviations between the precipitation totals of the lysimeters with different vegetation cover in SE are considerably low with CRs of 99.8–101.4 %.

405 **Table 5:** Precipitation sums (P) and catching ratios (CR) of all investigated gauges compared to the references per year. Only hours are considered, where all devices at a site were active, at least one device, tipping bucket (TB), weighable gauge (WG) or acoustic sensor (AS) and the lysimeters did measure a precipitation intensity of at least 0.1 mm h^{-1} and the precipitation is classified as "Rain".

Site	Year	n	P_{ref}	P_{lys_crop}	CR_{lys_crop}	P_{TB1}	CR_{TB1}	P_{TB2}	CR_{TB2}	P_{WG}	CR_{WG}	P_{AS}	CR_{AS}	P_{LD}	CR_{LD}
		(-)	(h)	(mm)	(mm)	(%)	(mm)	(%)	(mm)	(%)	(mm)	(%)	(mm)	(%)	(mm)	(%)
Rolles-broich	2015	793	709			334	47.1	594	83.8	606	85.5	499	70.4	676	95.3
	2016	989	801			184	22.9	634	79.2	659	82.2	526	65.6	687	85.7
	2017	1007	881			273	30.9	732	83.1	744	84.5	553	62.8	795	90.2
	2018	694	583			189	32.4	471	80.8	519	89.0	456	78.2	522	89.6
Sel-hausen	2015	736	599	600	100.1	244	40.7			549	91.7	423	70.6	589	98.4
	2016	697	554	556	100.3	221	39.9			495	89.4	388	70.0	455	82.1
	2017	581	431	430	99.8	169	39.2			398	92.3	303	70.2	317	73.6
	2018	548	388	394	101.4	79	20.4			367	94.5	319	82.1	373	96.1
Dedelow	2015	571	414			344	83.1					373	90.1		
	2016	641	423			322	76.1					351	83.1		
	2017	719	693			504	72.8					572	82.6		
	2018	407	279			235	84.0					255	91.3		

### 3.3 Precipitation intensities

410 On an hourly basis, all TBs tend to underestimate precipitation relative to the reference (Fig. 4). Measurements of the TBs showed little scattering, indicating consistent measurements with R²-values above or near 0.8 for all devices, except for TB1 in RO (Fig. 4 A2) with R² = 0.53. However, TB1 (RO; Fig. 4 A1) as well as the TB (SE; Fig. 4 C1) showed biases of -0.69 and -0.61 mm h^{-1} and SDDs of 0.90 and 0.85 mm h^{-1} for all rainfall events with $P_{ref} \geq 0.1$ mm h^{-1}. In hours of intensities between 0.1 to 2.5 mm h^{-1} the biases were -0.48 and -0.44 mm h^{-1} and the SDDs 0.40 and 0.38 mm h^{-1} (Fig. 4 A2 and C2).

415 Measurements from TB2 (RO; Fig. 4 B1) showed a bias of -0.18 mm h^{-1} and an SDD of 0.31 mm h^{-1} while the TB (DD; Fig. 4 D1) measures with a bias of -0.20 mm h^{-1} and an SDD of 0.41 mm h^{-1}. For slight precipitation intensities, measurements from TB2 (RO) had a bias of -0.16 mm h^{-1} and an SDD of 0.20 mm h^{-1} and TB (DD) a bias of -0.14 mm h^{-1} and an SDD of 0.2 mm h^{-1}, respectively (Fig. 4 B2 and D2).

Hydrology and
Earth System
Sciences
Discussions

Open Access
EGU
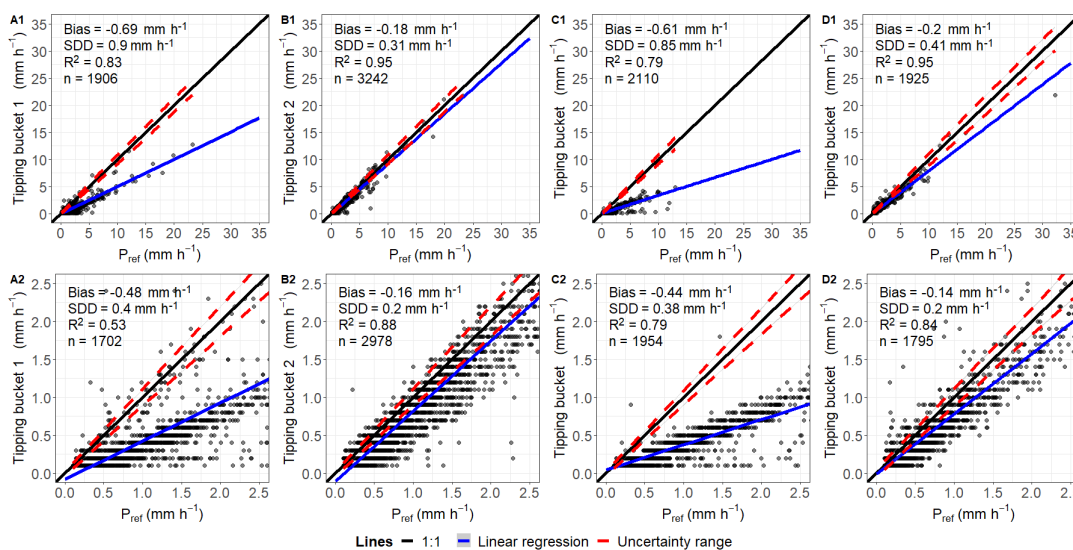
Figure 4: Comparison of hourly data determined by tipping buckets and lysimeters (P_{ref}) and classified as "Rain". Plots A1–D1 include all measurements taken where both P_{gauge} and P_{ref} are ≥ 0.1 mm h^{-1}. Plots A2–D2 show slight precipitation events and key values are calculated for P_{ref} between 0.1–2.5 mm h^{-1}. A1, A2: Rollesbroich lysimeter station. B1, B2: Rollesbroich EC station. C1, C2: Selhausen lysimeter station. D1, D2: Dedelow lysimeter station.

Measurements conducted by the WG (RO; Fig. 5 A1) showed a bias of -0.15 mm h^{-1} and an SDD of 0.24 mm h^{-1}. For the time without wind shield, measurements from the WG (SE; Fig. 5 B1) had a bias of -0.08 mm h^{-1} and an SDD of 0.18 mm h^{-1}, while with shield the bias was -0.04 mm h^{-1} and the SDD 0.14 mm h^{-1} (Fig. 5 C1). At $P_{ref} \leq 2.5$ mm h^{-1}, the bias decreased from 0.07 to 0.04 mm h^{-1} and the SDD from 0.16 to 0.12 mm h^{-1} after the installation of the wind shield (Fig. 5 B2 and C2) in comparison with the WG (RO; Fig. 5 A2) which's measurements for $P_{ref} \leq 2.5$ mm h^{-1} had a bias of -0.11 mm h^{-1} and an SDD of 0.16 mm h^{-1}.
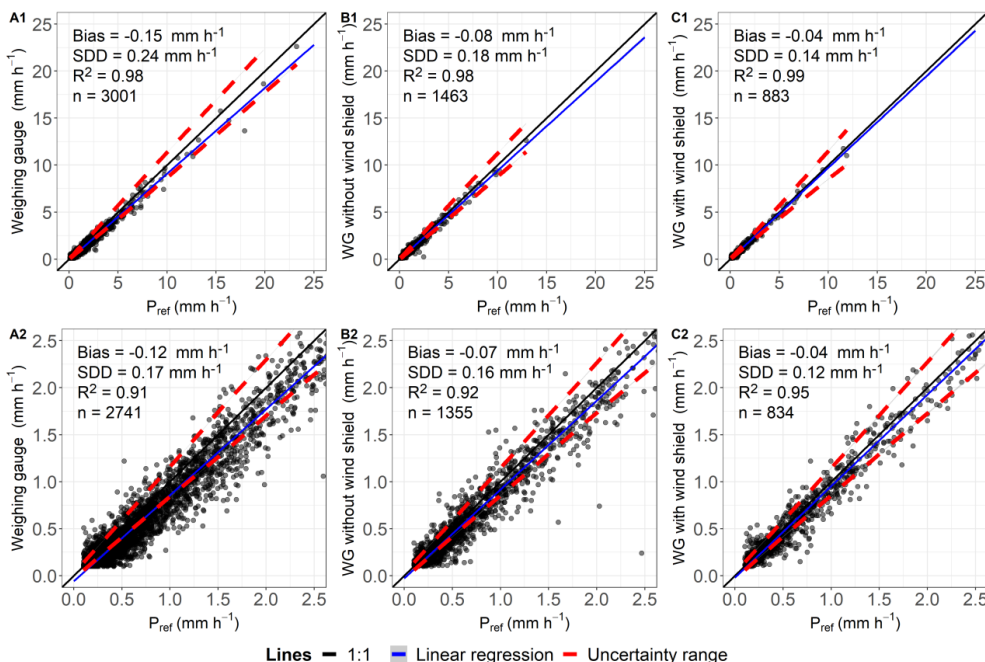
Figure 5: Comparison of hourly data determined by weighable gauges and lysimeters (P_{ref}) and classified as "Rain". Plots A1–C1 include all measurements taken with both P_{gauge} and P_{ref} are ≥ 0.1 mm h^{-1}. Plots A2–C2 show slight precipitation events and key values are calculated

for P_{ref} between 0.1–2.5 mm h^{-1}. A1, A2: Rollesbroich lysimeter station. B1, B2: Selhausen lysimeter station without installed wind shield around the weighable gauge. C1, C2: Selhausen lysimeter station with installed wind shield around the weighable gauge.

435   The ASs data scattered largely around the 1:1-line with the tendency of the ASs to underestimate the precipitation intensity (Fig. 6 A1 to C2). Especially for slight precipitation intensities, the measurements correlated poorly with the reference data. To exclude possible errors during the data processing, hourly values were calculated additionally, implementing a positive and negative 10-minutes lag on the data. This led to an even lower degree of agreement with the reference measurements, resulting in higher bias and SDDs than shown in Fig. 6. Additionally, a discrepancy between the measurement intervals from the ASs

440   and reference would also result in false positives because only sensor data would show precipitation. A plot with the data including P_{ref} = 0 (not shown here) reveals no suspicious occurrence of these false positives. Therefore, the data from the ASs was evaluated as valid. Measurements from the AS (RO; Fig. 6 A1) had a bias of -0.25 mm h^{-1} and an SDD of 0.7 mm h^{-1}. A bias of -0.22 mm h^{-1} and an SDD of 0.46 mm h^{-1} was calculated for $P_{ref} \leq 2.5$ mm h^{-1} (Fig. 6 A2). The R^2-value was 0.80 and 0.54, respectively. Measurements by the AS (SE) had a bias of -0.23 mm h^{-1}, an SDD of 0.57 mm h^{-1} and a R^2-value of 0.79

445   (Fig. 6 B1). For intensities classified as "slight", the sensor measured with a bias of -0.18 mm h^{-1}, an SDD of 0.37 mm h^{-1} and a R^2-value of 0.62 (Fig. 6 B2). The measurements from the AS in DD had a bias of 0.07 mm h^{-1} and an SDD of 0.66 mm h^{-1} with R^2 being 0.85 (Fig. 6 C1). Slight precipitation was measured with a bias of -0.07 mm h^{-1}, an SDD of 0.42 mm h^{-1} and a R^2-value of 0.60 (Fig. 6 C2).
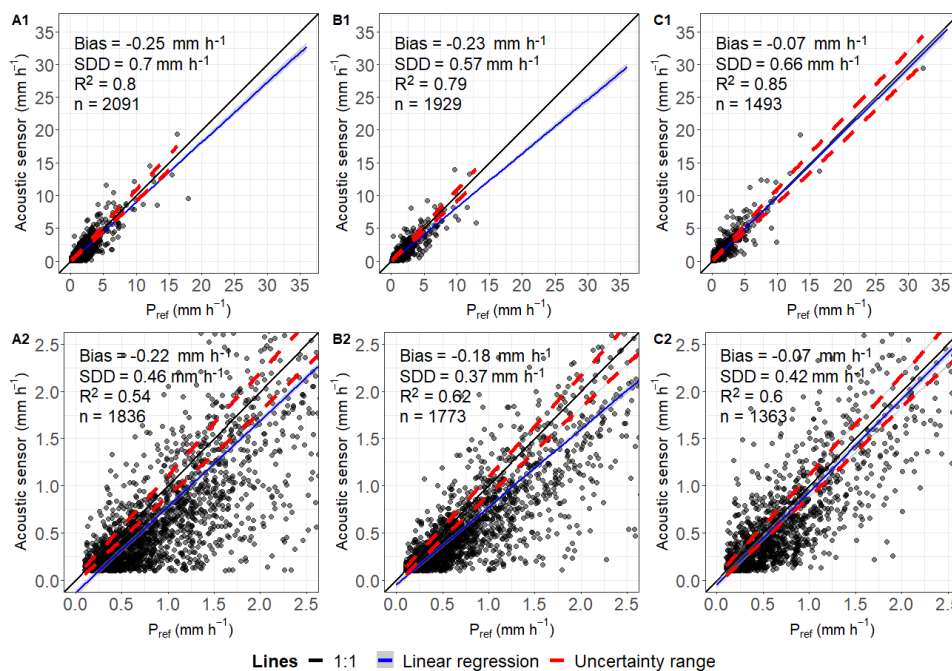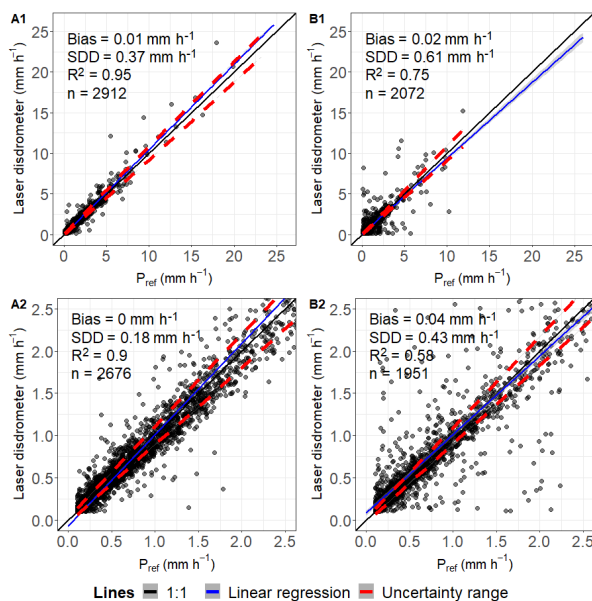

450

Figure 6: Comparison of hourly data determined by acoustic sensors and lysimeters (P_{ref}) and classified as "Rain". Plots A1–C1 include all measurements taken with both P_{gauge} and P_{ref} are ≥ 0.1 mm h^{-1}. Plots A2–C2 show slight precipitation events and key values are calculated for P_{ref} between 0.1–2.5 mm h^{-1}. A1, A2: Rollesbroich lysimeter station. B1, B2: Selhausen lysimeter station. C1, C2: Dedelow lysimeter station.

455   The LD (RO) tended to overestimate the precipitation with a general bias of 0.01 mm h^{-1} and an SDD of 0.37 mm h^{-1} (Fig. 7 A1). The R^2-value of 0.95 suggests a good correlation with the reference. For slight precipitation events, the bias was 0.00 mm h^{-1} with the SDD being 0.18 mm h^{-1} and R^2 0.90 (Fig. 7 A2).

The LD (SE) showed biases of 0.02 mm h^{-1} for all measurements and 0.04 mm h^{-1} for $P_{ref} < 2.50$ mm h^{-1} (Fig. 7 B1 and B2). The SDDs were 0.61 and 0.43 mm h^{-1} respectively. The R^2-values (0.75 and 0.58) were lower compared to the ones from the

Hydrology and
Earth System
Sciences
Discussions
Open Access
EGU

460   other disdrometer at RO. The number of recorded hours with precipitation occurring at both sides was higher for the plots with

the disdrometers compared to the plots of the other gauges due to the high measuring resolution of the disdrometer.


Figure 7: Comparison of hourly data determined by laser disdrometer and lysimeters (P_{ref}) and classified as "Rain". Plots A1–B1 include all measurements taken with both P_{gauge} and P_{ref} being ≥ 0.1 mm h^{-1}. Plots A2–B2 show slight precipitation events and key values are calculated
465   for P_{ref} between 0.1–2.5 mm h^{-1}. A1, A2: Rollesbroich lysimeter station. B1, B2: Selhausen lysimeter station.

3.4 Influence of wind speed

The CRs from TB1 (RO) and TB (SE) as functions of the wind speed at gauge height were mostly in the range of 30–100 %

and did not in- or decrease with increasing wind speed at gauge height (Fig. 8 A and C). A major influence of the wind on

hourly precipitation data therefore could not be identified. The CRs from TB2 (RO) showed a tendency to decrease at wind

470   speeds greater than 5 m s^{-1} (Fig. 8 B). In contrast, the CRs from TB (DD) tended to be above 100 % after the same threshold

and the regression line implies a positive correlation with the wind speed (Fig. 8 D). The CRs from the WGs did not exhibit

any correlation between the hourly precipitation data and the wind speed (Fig. 9 A to C), even with the separation according
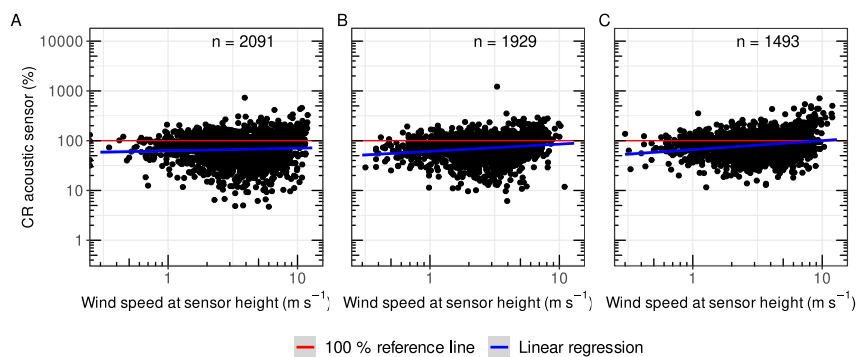
to the availability of the wind shield.
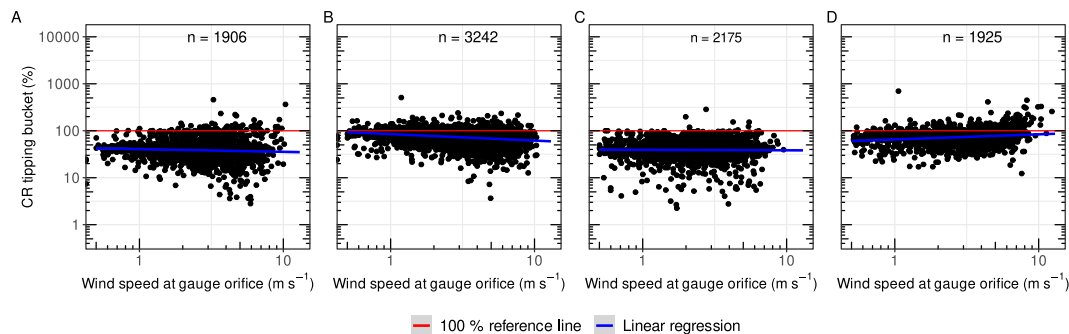
475   **Figure 8:** Catching ratios (CRs) of the tipping buckets as functions of the wind speed at gauge height for all sites, $P_{ref} \geq 0.1$ mm h^{-1} and precipitation classified as "Rain". A: Rollesbroich lysimeter station. B: Rollesbroich EC station. C: Selhausen lysimeter station. D: Dedelow lysimeter station.
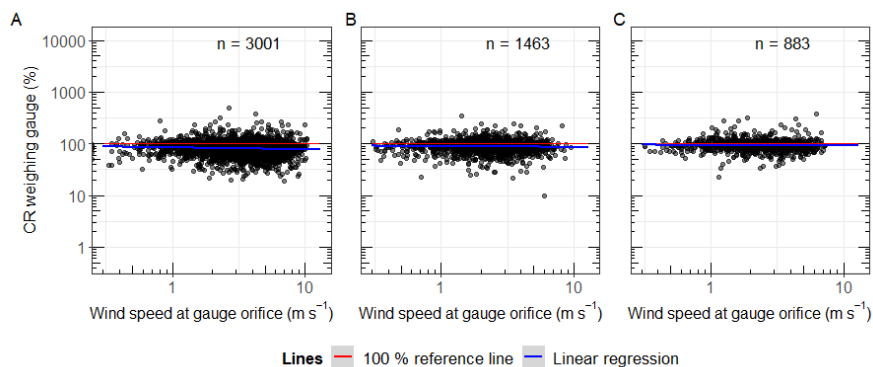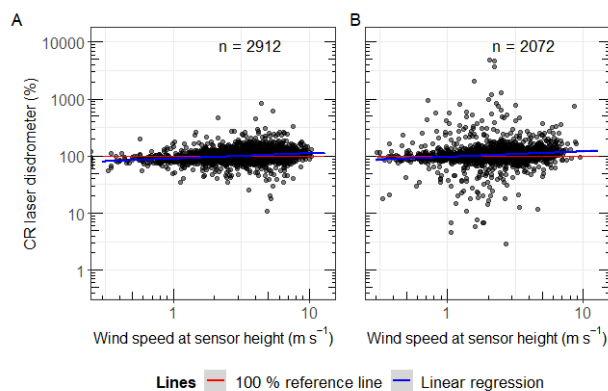
Figure 9: Catching ratios (CRs) of the weighable gauges as functions of the wind speed at gauge height, $P_{ref} \geq 0.1$ mm h^{-1} and precipitation classified as "Rain". A: Rollesbroich lysimeter station. B: Selhausen lysimeter station, before wind shield was installed. C: Selhausen lysimeter station, after wind shield was installed.

A slight increase of CRs at higher wind speeds could be traced back to an influence of the wind speed for the ASs at all sites (Fig. 10 A to C). The CRs of the LDs generally did not indicate dependencies on the wind speed at gauge height (Fig. 11 A to B). The CRs of the LD in SE generally spread to a greater extend around the 100 % reference line compared to LD in RO.

Figure 10. Catching ratios (CRs) of the acoustic sensors as functions of the wind speed at gauge height for all sites, $P_{ref} \geq 0.1$ mm h^{-1} and precipitation classified as "Rain". A: Rollesbroich lysimeter station. B: Selhausen lysimeter station. C: Dedelow lysimeter station.

Figure 11. Catching ratios (CRs) of the laser disdrometers as functions of the wind speed at gauge height for all sites, $P_{ref} \geq 0.1$ mm h^{-1} and precipitation classified as "Rain". A: Rollesbroich lysimeter station. B: Selhausen lysimeter station.

3.5 Precipitation correction

Applying the dynamic correction model (DCM) and the approach derived from Richter (1995) reduced the bias of all corrected measurements for the TBs and WGs (Table 6). Generally, the DCM resulted in a greater bias reduction than the other method. Both correction methods had no systematic effect on the SDD and R^2-values, but the CRs have been increased by 14 and 9 %

495 for the TBs and by 10 and 11% for the WGs due to the application of the DCM and method after Richter, respectively. The data correction also led to an increased number of hours exceeding the threshold of 0.1 mm h^{-1} for the WGs (Table 6 and 7). For the TBs, the aggregation of hourly to daily precipitation data during a processing step of the method derived from Richter resulted in a reduction of observations.

Table 6: Statistics of the corrected precipitation data classified as "Rain" for tipping bucket (TB) and weighable gauges (WG) at sites in
500 Rollesbroich (RO), Selhausen (SE) and Dedelow (DD). Due to the aggregation of hourly values and therefore the number of days with incomplete data as well as the threshold of 0.1 mm, which is met only after the correction, the number of observations (n) differed depending on the correction method. "Intercept" and "Slope" show the intercept and slope of the linear regression of P_{gauge} and P_{ref}.

Site	Device	Cor. method	Intercept	Slope	Bias	SDD	R^2	n
			(mm h^{-1})	(-)	(mm h^{-1})	(mm h^{-1})	(-)	(-)
	TB1	-	-0.08	0.50	-0.69	0.90	0.83	1906
	TB1	DCM	-0.01	0.47	-0.56	0.88	0.82	1906
	TB1	Richter	0.00	0.51	-0.61	0.90	0.83	1831
Rollesbroich	TB2	-	-0.11	0.93	-0.18	0.31	0.95	3242
	TB2	DCM	0.01	0.96	-0.03	0.30	0.95	3242
	TB2	Richter	-0.03	0.94	-0.09	0.30	0.95	3224
	TB	-	-0.04	0.33	-0.61	0.85	0.79	2110
Selhausen	TB	DCM	0.13	0.35	-0.51	0.83	0.78	2110
	TB	Richter	0.11	0.34	-0.54	0.85	0.78	2019
	TB	-	-0.01	0.79	-0.20	0.41	0.95	1925
Dedelow	TB	DCM	0.11	0.81	-0.06	0.42	0.93	1925
	TB	Richter	0.07	0.80	-0.11	0.41	0.94	1925
	WG	-	-0.06	0.91	-0.15	0.24	0.98	3001
Rollesbroich	WG	DCM	0.01	0.95	-0.04	0.22	0.98	3107
	WG	Richter	0.01	0.93	-0.06	0.23	0.98	3185
	WG	-	-0.02	0.95	-0.07	0.17	0.98	2346
Selhausen	WG	DCM	0.01	0.99	0.01	0.17	0.98	2439
	WG	Richter	0.05	0.97	0.03	0.16	0.98	2497

Table 7: Catching ratios (CRs) of corrected tipping bucket (TB) and weighable gauge (WG) data (DCM = Dynamic Correction Model;
505 RI = correction based on the method derived from Richter, 1995). Only numbers (n) of hours are considered, when all devices at a site were active and at least one device (TB, WG, AS) did measure precipitation (P) classified as "Rain" of at least 0.1 mm h^{-1}. Latter conditions are differently met after the correction with the two correction methods, resulting in divergent numbers of observations and associated P_{ref}.

Site	Year	n DCM	n RI	P_{ref} DCM	P_{ref} RI	CR_{TB1} DCM	CR_{TB1} RI	CR_{TB2} DCM	CR_{TB2} RI	CR_{WG} DCM	CR_{WG} RI
	(-)	(h)	(h)	(mm)	(mm)	(%)	(%)	(%)	(%)	(%)	(%)
	2015	799	801	710	693	57.8	53.0	99.9	92.2	97.4	94.0
Rollesbroich	2016	1009	1054	803	805	29.5	26.9	95.0	88.7	92.4	92.0
	2017	1027	1020	882	856	39.6	36.5	98.3	93.0	94.7	94.0
	2018	709	705	584	557	41.3	38.0	96.3	90.8	99.7	99.1
	2015	760	744	601.36	552.4	52.5	48.9			100.5	103.7
Selhausen	2016	721	733	556.31	529	51.4	48.1			97.3	100.8
	2017	598	616	432.88	411.6	51.3	48.0			99.6	105.5
	2018	570	611	389.81	391.6	28.8	25.8			104.5	107.5

Hydrology and
Earth System
Sciences
Open Access

EGU

Discussions

	2015	571	571	407.52	407.5	103.3	97.2
Dedelow	2016	641	641	410.68	410.7	97.2	91.8
	2017	719	719	682.1	682.1	87.5	83.1
	2018	407	407	271.31	271.3	106.7	100.9

4 Discussion

4.1 Lysimeter measurements, reference values and the influence of non-rainfall events

510   The uncertainty ranges of the reference values and the overall strong correlation between the intensity measurements of the lysimeters within a site (Appendix B) demonstrate, that under field conditions and different climates, the lysimeter measurements were in good agreement with each other over the entire observation period at all sites. The uncertainties of the reference values meet the requirements defined by the WMO (2018) for gauges used in the field. They decreased with increasing precipitation intensity, reaching a threshold of 5 % at about 1 to 2 mm h^{-1}, which was observed at all study sites and

515   regardless of the vegetation cover of the lysimeters. Additionally, lysimeter data at the sites showed R²-values of 1 with a maximum bias of 0.01 mm h^{-1} and a maximum SDD of 0.05 mm h^{-1} (Appendix B1 to B3), indicating a good correlation. Since lysimeter measurement uncertainties increase exponentially with decreasing precipitation intensity from $P_{ref} < 1$ mm h^{-1}, calculating an average intensity from multiple lysimeters seems necessary for these data. For long-term periods, uncertainties were probably less important because of the assumed normally distributed deviations from the average.

520   In total, when comparing the cumulated precipitation within a certain period, the lysimeters registered more precipitation than any other precipitation gauge. It could therefore be assumed that the lysimeter measurements and therefore the reference values are closer to the "true" precipitation than any of the other measuring method compared. However, comparing total precipitation amounts over long-term periods between the gauges and lysimeters, even if filtered carefully, might be biased because of non-rainfall events (NRE), which contributed to the recorded precipitation measured by the lysimeters. NREs which occurred

525   before, during or after a regular precipitation event within respective time interval were hence classified as precipitation, while other precipitation gauges did not record these. NRE could thus lead to overestimations of lysimeter precipitation intensities, although the average intensity of a NRE is small compared to the precipitation intensity (RO: 0.012 mm h^{-1}; SE: 0.009 mm h^{-1}; DD: 0.013 mm h^{-1}) and the distribution of NRE intensities (Fig. 12 A to C) indicated that these presumably did not heavily bias hours with regular precipitation. Applying these averages for NRE intensities on all hours which were investigated for the

530   comparison of precipitation totals (Table 6), only 0.7 % (RO), 0.6 % (SE) and 0.8 % (DD) of the total registered precipitation would have been attributed to NRE. This indicates a possibly small impact of NREs on the results of this study. However, NRE (i.e., dew, hoar frost and fog) can contribute a substantial amount of water for the ecosystem at the annual scale (Forstner et al., 2021; Groh et al., 2019), which demonstrates clearly that high-precision lysimeters are ideal tools measuring the different NRE of ecosystems. A higher temporal resolution of the data, possibly 10-min intervals, could help to temporally delineate

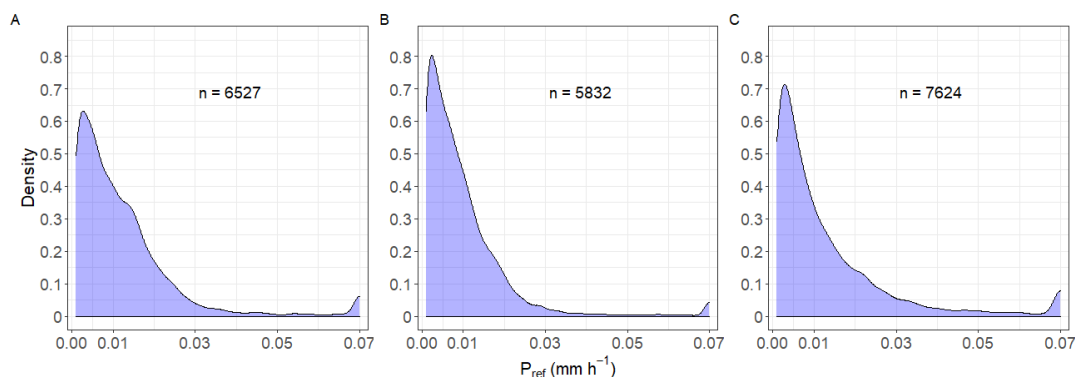535   precipitation events and NRE, as used by Groh et al. (2018b).

Figure 12: Distribution of water amounts formed during non-rainfall events ($P_{ref} > 0$ mm h^{-1}; $P_{gauge} = 0$ mm h^{-1}) occurring between sunset and sunrise. Hourly values of non-rainfall events were limited to a maximum value of 0.07 mm h^{-1} according to Monteith and Unsworth (2013). A: Rollesbroich lysimeter station. B: Selhausen lysimeter station. C: Dedelow lysimeter station.

4.2 Evaluation of gauge types for the comparison of precipitation data

The systematic deviations between the reference values and the precipitation intensity measurements by TB1 in RO (Fig. 4 A) and the TB in SE (Fig. 4 C) on one side and the better fitting data from TB2 (RO; Fig 5 B) and TB in DD (Fig. 4 D) on the other side, can only be explained by divergent calibrations. All TBs were of the same type and only differed in the equipped heating module, which did not affect the measurements compared, since it only worked at low temperatures and was intended to melt solid precipitation. The TB (DD) also had a greater catching surface area of 400 cm² compared to 200 cm² at other sites. However, this effect should be deducted by the internal processing. A spatial influence on the measurements was also unlikely since TB2 in RO was installed 30 m away from the lysimeter station and measured values closer to the reference than TB1, which was located only 5 m beside the lysimeters. The maintenance and service intervals were nearly equal at all sites. No or incorrect calibration could lead to a systematic underestimation of precipitation measurements, especially regarding TBs (Calder and Kidd, 1978; Niemczynowicz, 1986; Shedekar et al., 2016). If the precipitation amount of the internal processing software does not agree with the amount of liquid, which is poured by a tip of the bucket, the bias increases with the amounts of tips. Thus, an increased underestimation of the precipitation intensity can be recognized with increasing reference values. Kohfahl and Saaltink (2020) also found that TBs located at the same site differed in the amount of precipitation measured during six rain events compared to a high-precision weighable lysimeter for bare soil conditions. The authors assumed that the TB, which showed significant errors with minor amounts of rainfall, was affected by an individual technical problem. However, also the TB2 (RO; Fig. 4 D) showed a systematic underestimation of precipitation intensities, in particular for slight precipitation intensities. The TB (DD) was also prone to this circumstance and showed in addition outlier up to 9 mm h^{-1} at slight precipitation events. This might also be fixed with a dynamic calibration, although the occurrence of outliers towards an overestimation was exceptional compared to the other TBs. Considering that the hourly deviations led to underestimations of up to 67.7 % compared to the reference (TB RO; n = 3483 h), calibrations should be conducted regularly when operating a TB. TBs were also subject to the wetting loss, since precipitation can adhere on the gauge's inlet due to rough material surfaces and thus can be evaporated or sublimated without being measured (Sevruk, 1974). Due to the gauge's specific resolution, which is limited for TB gauges by the volume of a bucket, certain amounts of precipitation could not be registered and therefore got lost (loss of trace precipitation; Seibert and Morén, 1999; Sugiura et al., 2003; Yang et al., 1999b). This is particularly relevant because a minimum threshold of 0.1 mm h^{-1} can be set for the overall comparison, but precipitation amounts below or above the gauge's resolution were not recorded by the respective TBs, but only by the lysimeters. This could lead to an underestimation of precipitation amounts compared to the reference. In addition to other external influences such as wind and temperature, this is reflected in the slight, systematic underestimation of the better performing TBs.

Hydrology and
Earth System
Sciences
Discussions

Open Access
EGU

The WGs had the best correlation with low biases and small deviations in the precipitation totals, when the internally unprocessed data was compared to the reference. At both investigation sites, the devices underestimated the precipitation intensity consistently but within or close to the uncertainty range of the reference values. The weighable gauge (WG; RO) had a slightly lower R^2-value and SDD, which might go back to generally higher wind speeds at the site. The installation of the wind shield had a positive effect on reducing the bias and SDD of the WG (SE; Fig. 5). This results agreed well with a previous study which showed that Alter wind shield on a WG (Pluvio²) reduced the bias and increased the accuracy compared to an unshielded WG (Kochendorfer et al., 2017a). Overall, the WG also achieved the highest CR in the comparison of absolute precipitation at both sites. Here, too, there was a difference of 14.7–8.0 % compared to the reference, which could be explained by the gauge's resolution and the wind effect. These results generally support approaches from other studies (e.g., Fehlmann et al., 2020; Johannsen et al., 2020) that used the WG as a reference device to study other gauges. Although the deviations of the WG data from the lysimeter data were still relatively high, this was the best correlation of all the investigated gauges in this study.

The hourly precipitation intensities determined by the AS were inaccurate compared to the reference with both, over- and underestimated intensities, shown by SDDs of up to 0.7 mm h^{-1}. External or internal data processing implementing an artificial time lag would lead to similar broad scattering (Fig. 6). However the data were tested for known errors indicating a time lag and no such influence could be identified. Salmi and Ikonen (2005) pointed out, that variations of the AS measurements were more of a stochastic than systematic origin. Variation in the shape and velocity of the hydrometeors caused by air movements were the main reason for erroneous measurements. Stochastic errors were also produced by the surface wetness and construction of the sensor itself due to sensitivity variations over the sensor area. In a comparison of multiple instruments to measure precipitation, Liu et al. (2013) found the lowest correlation coefficient and the largest SD while comparing their reference, a TB, with the AS with a temporal resolution of one minute. Moreover, the AS overestimated the rainfall accumulation and recorded little higher rain intensity compared to their reference, when the rain intensity was less than 20 mm h^{-1} (Liu et al., 2013). According to Haselow et al. (2019), the AS showed overestimations by highly positive error values, compared to lysimeter reference data on a daily basis. Even though the hourly deviations in precipitation intensity were partly above the reference values, less absolute precipitation was measured by the ASs at all research sites than specified by the reference values. However, there were major differences between the sites. The different ASs in RO and SE registered 69.2 % and 73.2 % of the reference values, respectively, and in DD 86.8 %. The variation between the sites may exist due to the selection of hours with precipitation recorded by either the TB, AS or WG. The latter was absent in DD, so the threshold of 0.1 mm h^{-1} was more often reached by the AS at this site compared to the other sites. Therefore, precipitation registered only by the WG is not affecting the CRs of the ASs at DD.

Precipitation measurements performed by the LD had a small bias compared to the reference, which was probably primarily due to the resolution of the measuring device of 0.001 mm h^{-1}. The overall good correlations are reflected in the absolute values measured over a longer period, which can be compared with the CRs of the WGs. The deviations from the reference could be attributed to stochastic influences of drop size distributions and conversions during the processing of the measured data. According to a study by Johannsen et al. (2020), recorded drop sizes, velocity distributions, and kinetic energy intensity relationships were device-specific and showed similarities only for disdrometers of the same type across measurement sites. Liu et al. (2013) found that small raindrops tend to be omitted in larger size raindrops due to shadow effects of light. Also, two adjacent particles could appear as a large particle, resulting in wrong precipitation intensities (Lanzinger et al., 2006). The wind direction could also influence measurements of optical instruments as well as splashing of large raindrops off the device (Dengel et al., 2018). Hence an investigation of CRs as functions of the wind direction could reveal such interrelations. Furthermore, the number of erroneous measurements was high compared to the other gauges. For the LD (SE) 534 hours must be manually filtered, compared to 42 hours for the LD (RO). The data showed abrupt and isolated occurring hours with high precipitation intensities (> 50 mm h^{-1}) as well as consecutive hours with varying precipitation intensities, which were clearly

decoupled from actual precipitation events. This could be explained by foreign objects interfering with the laser beam. Additionally, prolonged time periods occurred when the disdrometer continuously recorded fluctuating precipitation intensities with notable deviations from the reference. This error might be triggered by spider webs or insects intercepting the laser, or

615 water and dust particles on the sensor, which were known to cause such errors on optical disdrometer measurements (Adirosi et al., 2018; Heyn et al., 2018).

Ultimately, all the gauges studied tended to underestimate precipitation amounts compared to the reference, both on an hourly basis and over longer time periods. This means that calibrating large-scale weather simulations with such biased gauge data could lead to an underestimation of actual precipitation amounts in these models. The use of a less accurate precipitation data

620 set in environmental model calibration compromises parameter identification and reduces the ability of the model to simulate processes associated with water and solute transport in the critical zone (e.g., Groh et al., 2018a). For the calculation of small-scale water balances, biased precipitation data as an input variable could also distort the overall research results.

4.3 Influence of wind speed on gauge precipitation measurements

Of the two best performing TBs, one (TB2, RO) exhibited generally lower CRs with increasing wind speed (Fig. 8 B). This

625 finding agreed with the general assumption of the effects of wind-field formations on Hellmann-design gauges (Sevruk et al., 1989). The TB (DD) revealed increased CRs at higher wind speeds (Fig. 8 D). Usually, the contrary effect is assumed (Duchon and Biddle, 2010; La Barbera et al., 2002). A connection of this phenomenon to the precipitation intensity was not evident. The AS at the site also had a higher CR than the reference at high wind speeds (Fig. 10 D), but this pattern occurred also at other sites (Fig. 10 B to D). The TB (DD) is the only TB installed directly within the crop field. Thus, during crop season,

630 water from the surrounding vegetation might have dripped into the funnel and the crop might have functioned as wind protection. However, a comparison of data from the respective months with (April–July) and without available crops does not indicate such an effect.

The CRs of the WG (RO) did not indicate significant influences of wind speed on the precipitation data (Fig. 9) even though the splitting of the WGs (SE) dataset according to the availability of a wind shield revealed such influences affecting the

635 measured precipitation intensities of the WGs. The CRs for the AS data might imply a bias towards overestimation of precipitation intensity with increasing wind speeds. This phenomenon was recognized in the literature (Liu et al., 2013) and could be traced back to the gauges measuring principle. An wind induced, increased terminal velocity with which a hydrometeor hits the sensors surface, was directly converted to higher precipitation intensities (Salmi and Ikonen, 2005). Both LD tended to have increased CRs along with higher wind speeds, which might be related to the conversion from recorded drop

640 size distribution and vertical velocity of the raindrops to precipitation intensities.

4.4 Evaluation of the precipitation data correction methods for TB and WG data

To improve data quality with precipitation data correction during post-processing, the correction method must be selected and adapted to the measuring device collecting the data (WMO, 2018). Here, two different correction methods were applied to TB and WG data to examine their impact on the respective hourly precipitation data. Both approaches reduced the bias of the TB

645 data relative to the reference, which was a key goal of the precipitation data correction. The dynamic correction model (DCM) led to a generally greater reduction of the bias (TBs: -0.13 mm h^{-1}; WGs: -0.09 mm h^{-1}) for all gauges than the approach derived from the method of Richter (1995; TBs: -0.08 mm h^{-1}; WGs: -0.07 mm h^{-1}). As a result of the corrections, considerable amounts of precipitation have been added to the precipitation totals in the period under study. Especially the correction of data from TB2 (RO), WG (RO) and WG (SE) led to CRs of 97.4 (+15.7 %), 96.0 (+10.7 %) and 100.5 % (+8.5 %) compared to the

650 lysimeter reference. This indicates that the correction methods showed the best effect for the data with the initially highest quality, but possibly could lead to overestimations, which was found in overcorrection of precipitation data for WG (Se; Table 7).

Haselow et al. (2019) used the linear scaling method to reduce the bias of daily precipitation data from multiple rain gauges compared to lysimeter measurements. To do this, they applied the ratio between the monthly rainfall totals from lysimeters and rain gauges to the daily rainfall totals of the rain gauges. The method successfully reduced the bias of the daily precipitation data despite for periods of high precipitation intensities (Haselow et al., 2019). However, a distinction must be made between correction methods that correct precipitation data solely on the basis of reference data (e.g., Fang et al., 2015) and methods such as the DCM used in this study that correct individual physical and technical induced errors like wind field deformation and evaporation. For the latter approach, the availability of results from comparable studies with weighable lysimeter references is limited. For TB1 (RO) and TB (SE), the correction was not sufficient to compensate for the systematic biases from the reference, although the distortion probably came from calibration issues that were not intended to be corrected by the DCM. An overcorrection of the precipitation intensities for the WGs at high wind speeds cannot be ruled out, especially since the Alter wind shield has already reduced the influence of the wind on the WG (SE). Michelson (2004) found that the DCM resulted in more accurate precipitation estimates, although uncertainties in the treatment of measurements for some gauge types remain, which can be confirmed by the results of this work. The results also showed that the biases for all corrected TBs were reduced by applying the adjusted correction method according to Richter (1995), although high biases still remain for the TB1 (RO), TB (SE) and TB (DD). It must be taken into account that the orders of magnitude of these correction amounts were detached from individual environmental influences at the sites and only related to the manual Hellmann type gauge (Richter, 1995). Richter (1995) also stated that due to the large daily variability of the individual error-causing parameters, the statistical error of the calculations based on mean ratios was inevitably large and mainly in the magnitude of the correction amount. Therefore, the adjustment to correct the hourly measurements increased the statistical error. Based on given data availability of reference, gauge, and weather data, machine learning algorithms might be a promising tool to further optimise device-specific precipitation data corrections.

5 Conclusions

Precipitation data from three research sites of the TERENO-SOILCan network based on high-precision weighable lysimeters were used as reference to investigate the functionality and data quality of four different precipitation measurement methods. The arithmetic mean of the lysimeter measurements has proven to be an almost unbiased reference for the precipitation measurement method. The results of this study revealed that each gauge-based method (i.e., tipping bucket gauges, weighable gauges, acoustical sensors, and optical laser disdrometers) was affected differently by wind, precipitation intensity, measurement resolution and technical errors. All precipitation measurement methods underestimated the precipitation amounts for the observation period with deviations of 8 % to 67 % from the reference if only hours with precipitation intensities greater than 0.1 mm h^{-1} were considered. This implies that point precipitation data should be treated as minimum values, especially when looking at cumulative totals over long time periods. When using hourly data for water balances or local projections of climate change, an uncertainty regarding over- and underestimation of point precipitation data must be taken into account, depending on the gauge type. The results confirmed that correction algorithms, which consider the influence of wind and other typical sources of error on the instruments, reduced the bias between reference and measurements and improved the catching ratios of hourly precipitation data from rain gauges (tipping bucket and weighable gauge) under different climatic conditions at three different TERENO-SOILCan test sites. The Dynamic Correction Model achieved higher average catch ratios compared to the correction approach derived from Richter. Therefore, only the Dynamic Correction Model might be the right tool to correct hourly precipitation data. Adequate reference data are crucial for testing and developing correction methods to overcome errors in precipitation measurements from standard point gauges. Observations from weighable, high-precision lysimeter (e.g., TERENO-SOILCan network) provide such data to improve estimates of point scale precipitation under different climatic conditions. Unbiased point-scale precipitation estimates are essential when estimating precipitation at larger

scales remotely from either ground-based weather radars or from satellites. Precipitation is the main driver of the hydrological

695   cycle and accurate data help to improve local weather and climate forecasts, which is particularly relevant in the context of

climate change.

Appendix A
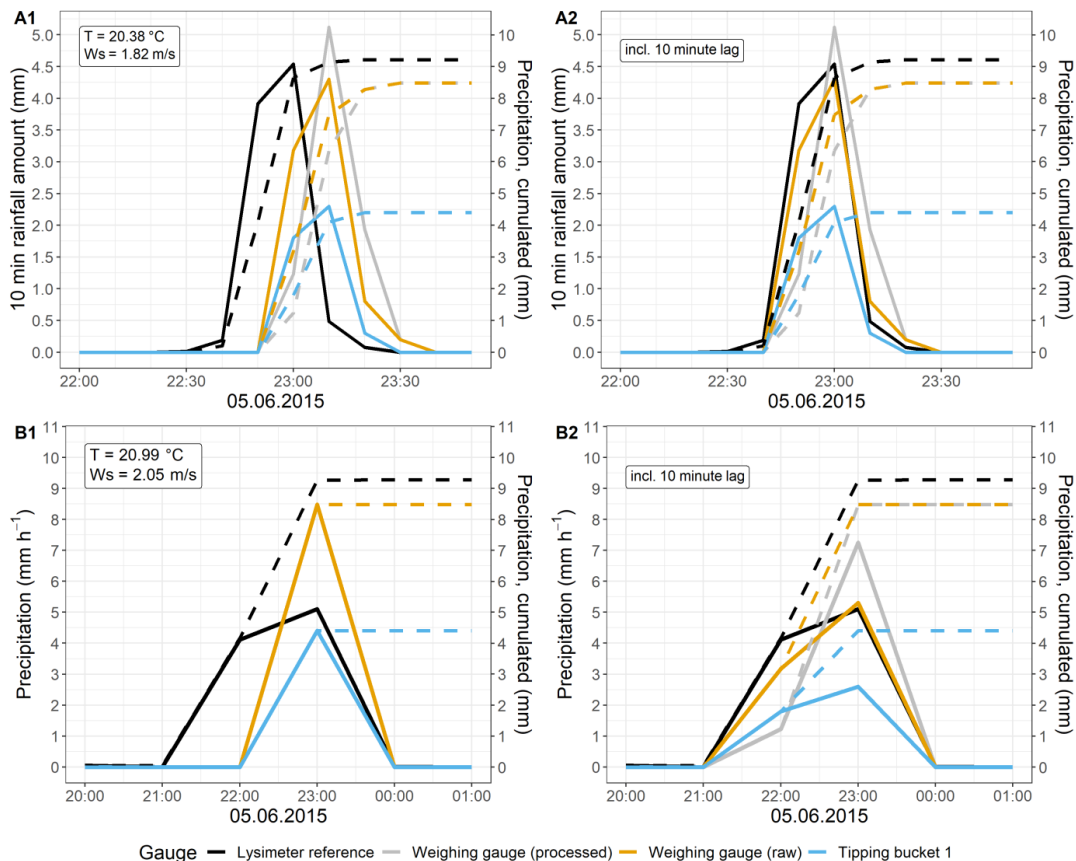
Figure A1: Time series of a precipitation event in Selhausen with a temporal resolution of A: 10 minutes, B: one hour. Solid lines display
700   the precipitation intensity (left y-axis) and dashed lines the cumulative precipitation (right y-axis). A1 and B1 show original data. A2 and
B2 show data with an implemented reverse time lag of 10 minutes for the tipping bucket and weighable gauge.

Appendix B
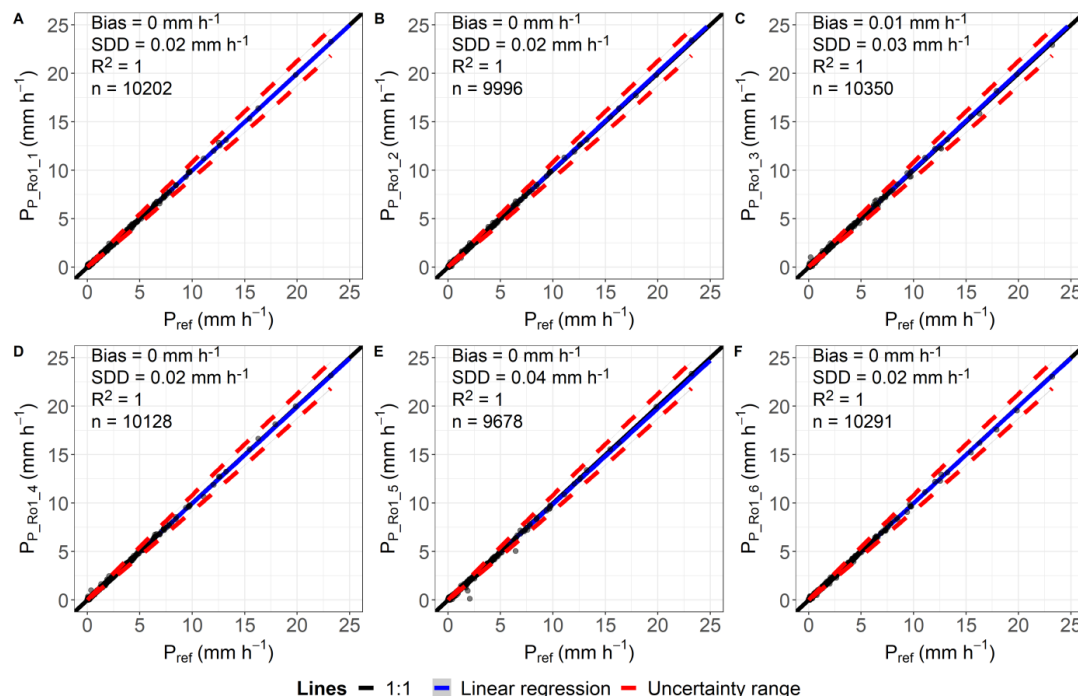
Figure B1: Comparison of hourly precipitation data classified as "Rain", determined by lysimeter and reference data (P_{ref}) for the lysimeter station in Rollesbroich. Plots A–F include all hours of measurements taken where both P_{lys} and P_{ref} are ≥ 0.001 mm h⁻¹. The vegetation grown on the lysimeter is of a grassland type.
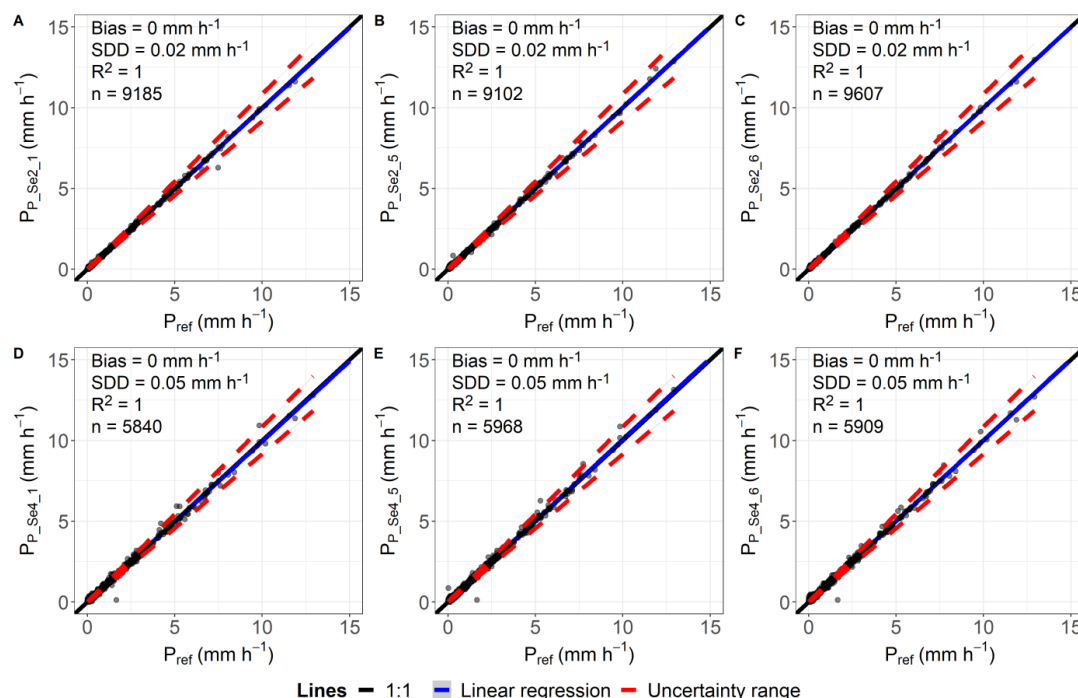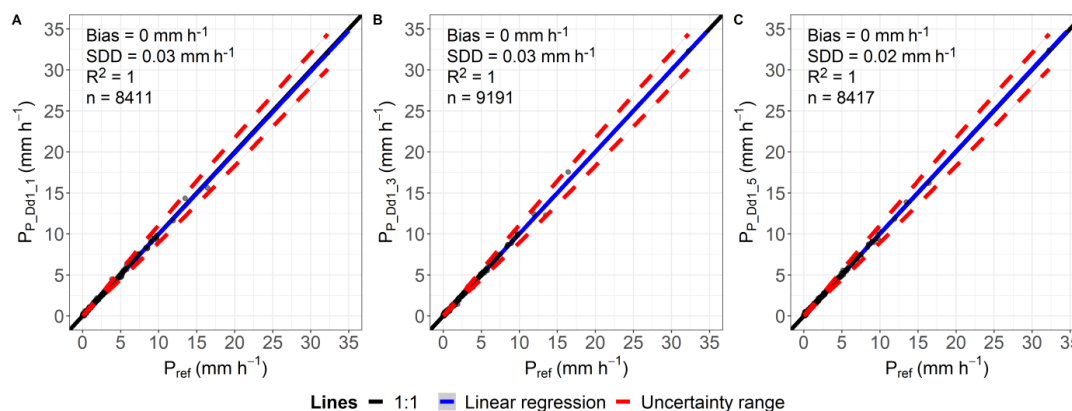

Figure B2: Comparison of hourly precipitation data classified as "Rain", determined by lysimeter and reference data (P_{ref}) for the lysimeter station in Selhausen. Plots A–C include all hours of measurements taken where both P_{lys} and P_{ref} are ≥ 0.001 mm h⁻¹ and the vegetation

710   grown on the lysimeter is of a grassland type. Plots D–F include all hours of measurements taken where both P_{lys} and P_{ref} are ≥ 0.001 mm h^{-1}
and the vegetation grown on the lysimeter is of an arable land type.

Figure B3: Comparison of hourly precipitation data classified as "Rain", determined by lysimeter and reference data (P_{ref}) for the lysimeter
station in Dedelow. Plots A–C include all hours of measurements taken where both P_{lys} and P_{ref} are ≥ 0.001 mm h^{-1}. The vegetation grown
715   on the lysimeter is of an arable land type.

Data availability

All raw data for the specific lysimeters, precipitation gauges and weather stations from Rollesbroich and Selhausen can be
freely obtained from the TERENO data portal (https://teodoor.icg.kfa-juelich.de/ddp/index.jsp (last access: 20 October 2022;
Kunkel et al., 2013) with respective ID codes.

720   Rollesbroich lysimeter station: RO_BKY_010 (gauge and weather data), RO_Y_01 (lysimeter data).

Rollesbroich Eddy covariance station: RO_EC_001 (gauge data).

Selhausen lysimeter station: SE_BDK_002 (gauge and weather data), SE_Y_02 (lysimeter: Se_Y_021, Se_Y_025,
Se_Y_026), SE_Y_04 (lysimeter: Se_Y_041, Se_Y_045, Se_Y_046).

Dedelow lysimeter station: Dd_K_01 (gauge and weather data), Dd_Y_01 (lysimeter data). The data for the experimental
725   station in Dedelow can be acquired upon request from Jannis Groh.

Author contributions

TP conceived the experiments. JG, TP, and TS had the idea and designed the study. JG provided the data for the corresponding
lysimeter stations. HHG and BR guided the conceptualization and the internal review process. TS performed the data analysis
and wrote the paper with equal contributions from all co-authors.

730   **Competing interests**

The authors declare that they have no conflict of interest.

Acknowledgements

Hydrology and
Earth System
Sciences
Discussions

References

Adirosi, E., Roberto, N., Montopoli, M., Gorgucci, E., and Baldini, L.: Influence of Disdrometer Type on Weather Radar
Algorithms from Measured DSD: Application to Italian Climatology, Atmosphere, 9, 360,
740   https://doi.org/10.3390/atmos9090360, 2018.

Alter, J. C.: Shielded storage precipitation gages, Mon. Wea. Rev., 65, 1520-0493, https://doi.org/10.1175/1520-
0493(1937)65%3C262:SSPG%3E2.0.CO;2, 1937.

Bárdossy, A., Kilsby, C., Birkinshaw, S., Wang, N., and Anwar, F.: Is Precipitation Responsible for the Most Hydrological
Model Uncertainty?, Front. Water, 4, https://doi.org/10.3389/frwa.2022.836554, 2022.

745 Bloemink, H. I. and Lanzinger, E.: Precipitation type from the Thies disdrometer, WMO, Bukarest, 2005.

Bogena, H. R., Montzka, C., Huisman, J. A., Graf, A., Schmidt, M., Stockinger, M., Hebel, C. von, Hendricks-Franssen, H.
J., van der Kruk, J., Tappe, W., Lücke, A., Baatz, R., Bol, R., Groh, J., Pütz, T., Jakobi, J., Kunkel, R., Sorg, J., and
Vereecken, H.: The TERENO-Rur Hydrological Observatory: A Multiscale Multi-Compartment Research Platform for
the Advancement of Hydrological Science, Vadose Zone Journal, 17, 180055, https://doi.org/10.2136/vzj2018.03.0055,
750   2018.

Calder, I. R. and Kidd, C.: A note on the dynamic calibration of tipping-bucket gauges, Journal of Hydrology, 39, 383–386,
https://doi.org/10.1016/0022-1694(78)90013-6, 1978.

Chen, R., Liu, J., Kang, E., Yang, Y., Han, C., Liu, Z., Song, Y., Qing, W., and Zhu, P.: Precipitation measurement
intercomparison in the Qilian Mountains, north-eastern Tibetan Plateau, The Cryosphere, 9, 1995–2008,
755   https://doi.org/10.5194/tc-9-1995-2015, 2015.

Chvíla, B., Sevruk, B., and Ondrás, M.: The wind-induced loss of thunderstorm precipitation measurements, Atmospheric
Research, 77, 29–38, https://doi.org/10.1016/j.atmosres.2004.11.032, 2005.

Dengel, S., Graf, A., Grünwald, T., Hehn, M., Kolari, P., Löfvenius, M. O., Merbold, L., Nicolini, G., and Pavelka, M.:
Standardized precipitation measurements within ICOS: rain, snowfall and snow depth: a review, International
760   Agrophysics, 32, 607–617, https://doi.org/10.1515/intag-2017-0046, 2018.

Duchon, C. E. and Biddle, C. J.: Undercatch of tipping-bucket gauges in high rain rate events, Adv. Geosci., 25, 11,
https://doi.org/10.5194/adgeo-25-11-2010, 2010.

Duchon, C. E. and Essenberg, G. R.: Comparative rainfall observations from pit and aboveground rain gauges with and
without wind shields, Water Resour. Res., 37, 3253–3263, https://doi.org/10.1029/2001WR000541, 2001.

765 DWD: Niederschlag: vieljährige Mittelwerte 1961 - 1990, Deutscher Wetterdienst,
https://www.dwd.de/DE/leistungen/klimadatendeutschland/mittelwerte/nieder_6190_akt_html.html?view=nasPublicatio
n&nn=16102, last access: 8 October 2021, 2021a.

DWD: Temperatur: vieljährige Mittelwerte 1961 - 1990, Deutscher Wetterdienst,
https://www.dwd.de/DE/leistungen/klimadatendeutschland/mittelwerte/temp_6190_akt_html.html?view=nasPublication
770   &nn=16102, last access: 8 October 2021, 2021b.

Fang, G. H., Yang, J., Chen, Y. N., and Zammit, C.: Comparing bias correction methods in downscaling meteorological
variables for a hydrologic impact study in an arid area in China, Hydrol. Earth Syst. Sci., 19, 2547–2559,
https://doi.org/10.5194/hess-19-2547-2015, 2015.

Fehlmann, M., Rohrer, M., Lerber, A. von, and Stoffel, M.: Automated precipitation monitoring with the Thies disdrometer:
775   biases and ways for improvement, Atmos. Meas. Tech., 13, 4683–4698, https://doi.org/10.5194/amt-13-4683-2020,
2020.

Førland, E. J., Allerup, P., Dahlström, B., Elomaa, E., Jónsson, T., Madsen, H., Perälä, J., Rissanen, P., Vedin, H., and
Vejen, F.: Manual for Operational Correction of Nordic Precipitation Data, Oslo, 1996.

Hydrology and
Earth System
Sciences
Discussions

Open Access

EGU

Forstner, V., Groh, J., Vremec, M., Herndl, M., Vereecken, H., Gerke, H. H., Birk, S., and Pütz, T.: Response of water fluxes

780   and biomass production to climate change in permanent grassland soil ecosystems, Hydrol. Earth Syst. Sci., 25, 6087–
        6106, https://doi.org/10.5194/hess-25-6087-2021, 2021.

Fuchs, T., Rapp, J., Rubel, F., and Rudolf, B.: Correction of synoptic precipitation observations due to systematic measuring
        errors with special regard to precipitation phases, Physics and Chemistry of the Earth, Part B: Hydrology, Oceans and
        Atmosphere, 26, 689–693, https://doi.org/10.1016/S1464-1909(01)00070-3, 2001.

785 Gebler, S., Hendricks Franssen, H.-J., Kollet, S. J., Qu, W., and Vereecken, H.: High resolution modelling of soil moisture
        patterns with TerrSysMP: A comparison with sensor network data, Journal of Hydrology, 547, 309–331,
        https://doi.org/10.1016/j.jhydrol.2017.01.048, 2017.

Gebler, S., Hendricks Franssen, H.-J., Pütz, T., Post, H., Schmidt, M., and Vereecken, H.: Actual evapotranspiration and
        precipitation measured by lysimeters: a comparison with eddy covariance and tipping bucket, Hydrol. Earth Syst. Sci.,

790   19, 2145–2161, https://doi.org/10.5194/hess-19-2145-2015, 2015.

Goodison, B. E., Louie, P., and Yang, D.: WMO Solid Precipitation Measurement Intercomparison, Final Report, World
        Meteorological Organization, Instruments and observing methods, 67, 1998.

Goss, M. J. and Ehlers, W.: The role of lysimeters in the development of our understanding of soil water and nutrient
        dynamics in ecosystems, Soil Use and Management, 25, 213–223, https://doi.org/10.1111/j.1475-2743.2009.00230.x,

795   2009.

Groh, J., Pütz, T., Gerke, H. H., Vanderborght, J., and Vereecken, H.: Quantification and Prediction of Nighttime
        Evapotranspiration for Two Distinct Grassland Ecosystems, Water Resour. Res., 55, 2961–2975,
        https://doi.org/10.1029/2018WR024072, 2019.

Groh, J., Diamantopoulos, E., Duan, X., Ewert, F., Herbst, M., Holbak, M., Kamali, B., Kersebaum, K.-C., Kuhnert, M.,

800   Lischeid, G., Nendel, C., Priesack, E., Steidl, J., Sommer, M., Pütz, T., Vereecken, H., Wallor, E., Weber, T. K.,
        Wegehenkel, M., Weihermüller, L., and Gerke, H. H.: Crop growth and soil water fluxes at erosion-affected arable sites:
        Using weighing lysimeter data for model intercomparison, Vadose Zone Journal, 19, https://doi.org/10.1002/vzj2.20058,
        2020a.

Groh, J., Vanderborght, J., Pütz, T., Vogel, H.-J., Gründling, R., Rupp, H., Rahmati, M., Sommer, M., Vereecken, H., and

805   Gerke, H. H.: Responses of soil water storage and crop water use efficiency to changing climatic conditions: a lysimeter-
        based space-for-time approach, Hydrol. Earth Syst. Sci., 24, 1211–1225, https://doi.org/10.5194/hess-24-1211-2020,
        2020b.

Groh, J., Stumpp, C., Lücke, A., Pütz, T., Vanderborght, J., and Vereecken, H.: Inverse Estimation of Soil Hydraulic and
        Transport Parameters of Layered Soils from Water Stable Isotope and Lysimeter Data, Vadose Zone Journal, 17,

810   170168, https://doi.org/10.2136/vzj2017.09.0168, 2018a.

Groh, J., Slawitsch, V., Herndl, M., Graf, A., Vereecken, H., and Pütz, T.: Determining dew and hoar frost formation for a
        low mountain range and alpine grassland site by weighable lysimeter, Journal of Hydrology, 563, 372–381,
        https://doi.org/10.1016/j.jhydrol.2018.06.009, 2018b.

Hagenau, J., Meissner, R., and Borg, H.: Effect of exposure on the water balance of two identical lysimeters, Journal of

815   Hydrology, 520, 69–74, https://doi.org/10.1016/j.jhydrol.2014.11.030, 2015.

Hannes, M., Wollschläger, U., Schrader, F., Durner, W., Gebler, S., Pütz, T., Fank, J., Unold, G. von, and Vogel, H.-J.: A
        comprehensive filtering scheme for high-resolution estimation of the water balance components from high-precision
        lysimeters, Hydrol. Earth Syst. Sci., 19, 3405–3418, https://doi.org/10.5194/hess-19-3405-2015, 2015.

Haselow, L., Meissner, R., Rupp, H., and Miegel, K.: Evaluation of precipitation measurements methods under field

820   conditions during a summer season: A comparison of the standard rain gauge with a weighable lysimeter and a

piezoelectric precipitation sensor, Journal of Hydrology, 575, 537–543, https://doi.org/10.1016/j.jhydrol.2019.05.065, 2019.

Heinrich, I., Balanzategui, D., Bens, O., Blasch, G., Blume, T., Böttcher, F., Borg, E., Brademann, B., Brauer, A., Conrad, C., Dietze, E., Dräger, N., Fiener, P., Gerke, H. H., Güntner, A., Heine, I., Helle, G., Herbrich, M., Harfenmeister, K.,
825   Heußner, K.-U., Hohmann, C., Itzerott, S., Jurasinski, G., Kaiser, K., Kappler, C., Koebsch, F., Liebner, S., Lischeid, G., Merz, B., Missling, K. D., Morgner, M., Pinkerneil, S., Plessen, B., Raab, T., Ruhtz, T., Sachs, T., Sommer, M., Spengler, D., Stender, V., Stüve, P., and Wilken, F.: Interdisciplinary Geo-ecological Research across Time Scales in the Northeast German Lowland Observatory (TERENO-NE), Vadose Zone Journal, 17, 180116, https://doi.org/10.2136/vzj2018.06.0116, 2018.

830   Herbrich, M. and Gerke, H. H.: Autocorrelation analysis of high resolution weighing lysimeter time series as a basis for determination of precipitation, Z. Pflanzenernähr. Bodenk., 179, 784–798, https://doi.org/10.1002/jpln.201600169, 2016.

Hertel, C. and Unold, G. von: Third-generation lysimeters: scientific engineered monitoring systems., in: Novel measurement and assessment tools for monitoring and management of land and water resources in agricultural landscapes of central Asia., edited by: Mueller, L., Saparov, A., and Lischeid, G., Springer International Cham,
835   Heidelberg, New York, Dordrecht, London, 175–184, https://doi.org/10.1007/978-3-319-01017-5_9, 2013.

Heyn, K., Lönnqvist, J., and Linna, T.: Uncertainty sources that limit the precipitation identification / quantification ad extinction coefficient determination capabilities of optical present weather and visibility sensors, in: WMO Technical Conference on Meteorological and Environmental Instruments and Methods of Observation, Amsterdam, the Netherlands, October 8th - 11th 2018, 2018.

840   Hoffmann, M., Schwartengräber, R., Wessolek, G., and Peters, A.: Comparison of simple rain gauge measurements with precision lysimeter data, Atmospheric Research, 174-175, 120–123, https://doi.org/10.1016/j.atmosres.2016.01.016, 2016.

Johannsen, L. L., Zambon, N., Strauss, P., Dostal, T., Neumann, M., Zumr, D., Cochrane, T. A., Blöschl, G., and Klik, A.: Comparison of three types of laser optical disdrometers under natural rainfall conditions, Hydrological sciences journal = Journal des sciences hydrologiques, 65, 524–535, https://doi.org/10.1080/02626667.2019.1709641, 2020.
845
Kochendorfer, J., Nitu, R., Wolff, M., Mekis, E., Rasmussen, R., Baker, B., Earle, M. E., Reverdin, A., Wong, K., Smith, C. D., Yang, D., Roulet, Y.-A., Buisan, S., Laine, T., Lee, G., Aceituno, J. L. C., Alastrué, J., Isaksen, K., Meyers, T., Brækkan, R., Landolt, S., Jachcik, A., and Poikonen, A.: Errors and adjustments for single-Alter shielded and unshielded weighing gauge precipitation measurements from WMO-SPICE, 2017a.

850   Kochendorfer, J., Rasmussen, R., Wolff, M., Baker, B., Hall, M. E., Meyers, T., Landolt, S., Jachcik, A., Isaksen, K., Brækkan, R., and Leeper, R.: The quantification and correction of wind-induced precipitation measurement errors, Hydrol. Earth Syst. Sci., 21, 1973–1989, https://doi.org/10.5194/hess-21-1973-2017, 2017b.

Kohfahl, C. and Saaltink, M. W.: Comparing precision lysimeter rainfall measurements against rain gauges in a coastal dune belt, Spain, Journal of Hydrology, 591, 125580, https://doi.org/10.1016/j.jhydrol.2020.125580, 2020.

855   Kunkel, R., Sorg, J., Klump, J., Kolditz, O., Rink, K., Gasche, R., and Neidl, F.: TEODOOR - A Spatial Data Infrastructure for terrestrial observation data, in: 2013 10th IEEE International Conference on Networking, Sensing and Control (ICNSC 2013): Evry, France, 10 - 12 April 2013, Evry, 4/10/2013 - 4/12/2013, 242–245, 2013.

La Barbera, P., Lanza, L. G., and Stagi, L.: Tipping bucket mechanical errors and theirs influence on rainfall statistics and extremes, Water Science and Technology, 45, 1–9, https://doi.org/10.2166/wst.2002.0020, 2002.

860   Lanza, L. G. and Vuerich, E.: The WMO Field Intercomparison of Rain Intensity Gauges, Atmospheric Research, 94, 534–543, https://doi.org/10.1016/j.atmosres.2009.06.012, 2009.

Lanzinger, E., Theel, M., and Windolph, H.: Rainfall Amount and Intensity measured by the Thies Laser Precipitation Monitor, TECO-2006, Geneva, Switzerland, 2006.

Liu, X. C., Gao, T. C., and Liu, L.: A comparison of rainfall measurements from multiple instruments, Atmos. Meas. Tech., 6, 1585–1595, https://doi.org/10.5194/amt-6-1585-2013, 2013.

865

Marek, G., Evett, S., Gowda, P. H., Howell, T. A., Copeland, K. S., and Baumhardt, R. L.: Post-Processing Techniques for Reducing Errors in Weighing Lysimeter Evapotranspiration (ET) Datasets, Trans.ASABE, 499–515, https://doi.org/10.13031/trans.57.10433, 2014.

McGuiness, J. L.: A comparison of lysimeter catch and rain gage catch, Agricultural Research Service, 124, 1966.

870

Meissner, R., Seeger, J., Rupp, H., Seyfarth, M., and Borg, H.: Measurement of dew, fog, and rime with a high-precision gravitation lysimeter, Z. Pflanzenernähr. Bodenk., 170, 335–344, https://doi.org/10.1002/jpln.200625002, 2007.

Michaelides, S., Levizzani, V., Anagnostou, E., Bauer, P., Kasparis, T., and Lane, J. E.: Precipitation: Measurement, remote sensing, climatology and modeling, Atmospheric Research, 94, 512–533, https://doi.org/10.1016/j.atmosres.2009.08.017, 2009.

875

Michelson, D. B.: Systematic correction of precipitation gauge observations using analyzed meteorological variables, Journal of Hydrology, 290, 161–177, https://doi.org/10.1016/j.jhydrol.2003.10.005, 2004.

Monteith, J. L. and Unsworth, M. H.: Principles of environmental physics: Plants, animals, and the atmosphere, 4. ed., Elsevier/Acad. Press, Amsterdam, 401 pp., 2013.

Morgan, D. L. and Lourence, F. J.: Comparison Between Rain Gage and Lysimeter Measurements, Water Resour. Res., 5,

880

724–728, https://doi.org/10.1029/WR005i003p00724, 1969.

Niemczynowicz, J.: The Dynamic Calibration of Tipping-Bucket Raingauges, Hydrology Research, 17 (3), 203–214, https://doi.org/10.2166/nh.1986.0013, 1986.

Nipher, F. E.: On the determination of the true rainfall, by elevated gages., Proceedings of the American Association for the Advancement of Science, 103–108, 1878.

885

Nolz, R., Kammerer, G., and Cepuder, P.: Interpretation of lysimeter weighing data affected by wind, Z. Pflanzenernähr. Bodenk., 176, 200–208, https://doi.org/10.1002/jpln.201200342, 2013.

Peters, A., Nehls, T., Schonsky, H., and Wessolek, G.: Separating precipitation and evapotranspiration from noise – a new filter routine for high-resolution lysimeter data, Hydrol. Earth Syst. Sci., 18, 1189–1198, https://doi.org/10.5194/hess-18-1189-2014, 2014.

890

Peters, A., Groh, J., Schrader, F., Durner, W., Vereecken, H., and Pütz, T.: Towards an unbiased filter routine to determine precipitation and evapotranspiration from high precision lysimeter measurements, Journal of Hydrology, 549, 731–740, https://doi.org/10.1016/j.jhydrol.2017.04.015, 2017.

Peters, A., Nehls, T., and Wessolek, G.: Technical note: Improving the AWAT filter with interpolation schemes for advanced processing of high resolution data, Hydrol. Earth Syst. Sci., 20, 2309–2315, https://doi.org/10.5194/hess-20-

895

2309-2016, 2016.

Pollock, M. D., O'Donnell, G., Quinn, P., Dutton, M., Black, A., Wilkinson, M. E., Colli, M., Stagnaro, M., Lanza, L. G., Lewis, E., Kilsby, C. G., and O'Connell, P. E.: Quantifying and Mitigating Wind-Induced Undercatch in Rainfall Measurements, Water Resour. Res., 54, 3863–3875, https://doi.org/10.1029/2017WR022421, 2018.

Porporato, A. and Rodriguez-Iturbe, I.: Ecohydrology-a challenging multidisciplinary research perspective, Hydrological

900

Sciences Journal, 47, 811–821, https://doi.org/10.1080/02626660209492985, available at: https://www.scopus.com/inward/record.uri?eid=2-s2.0-0036791266&doi=10.1080%2f02626660209492985&partnerID=40&md5=5cff77e1aeba7e0214fcca5d7fe5c047, 2002.

Pütz, T., Kiese, R., Wollschläger, U., Groh, J., Rupp, H., Zacharias, S., Priesack, E., Gerke, H. H., Gasche, R., Bens, O., Borg, E., Baessler, C., Kaiser, K., Herbrich, M., Munch, J.-C., Sommer, M., Vogel, H.-J., Vanderborght, J., and

905

Vereecken, H.: TERENO-SOILCan: a lysimeter-network in Germany observing soil processes and plant diversity influenced by climate change, Environ Earth Sci, 75, https://doi.org/10.1007/s12665-016-6031-5, 2016.

R Core Team: R: A language and environment for statistical computing., R Foundation for Statistical Computing, Vienna, Austria, 2020.

Richter, D.: Ergebnisse methodischer Untersuchungen zur Korrektur des systematischen Meßfehlers des Hellmann-Niederschlagsmessers., Berichte des Deutschen Wetterdienstes, Selbstverlag des Deutschen Wetterdienstes, Offenbach am Main, Berichte des Deutschen Wetterdienstes, 194, 1995.

Ross, A., Smith, C. D., and Barr, A.: An improved post-processing technique for automatic precipitation gauge time series, Atmos. Meas. Tech., 13, 2979–2994, https://doi.org/10.5194/amt-2019-423, 2020.

Ryu, S., Lee, G., Nitu, R., Smith, C., Lim, E., and Kim, H. L.: Quantitative comparison of two types of working field reference systems for the measurement of precipitation amount (R2), in: Proceedings of the WMO Technical Conference on Meteorological and Environmental Instruments and Methods of Observation Madrid, Spain, 2016.

Salmi, A. and Ikonen, J.: Piezoelectic precipitation sensor from Vaisala, in: WMO Technical Conference on Instruments and Methods of Observation (TECO-2005), Bucharest, Romania, 4–7, 2005.

Schneider, J., Groh, J., Pütz, T., Helmig, R., Rothfuss, Y., Vereecken, H., and Vanderborght, J.: Prediction of soil evaporation measured with weighable lysimeters using the FAO Penman–Monteith method in combination with Richards' equation, Vadose Zone Journal, https://doi.org/10.1002/vzj2.20102, 2021.

Schrader, F., Durner, W., Fank, J., Gebler, S., Pütz, T., Hannes, M., and Wollschläger, U.: Estimating Precipitation and Actual Evapotranspiration from Precision Lysimeter Measurements, Procedia Environmental Sciences, 19, 543–552, https://doi.org/10.1016/j.proenv.2013.06.061, 2013.

Seibert, J. and Morén, A.-S.: Reducing systematic errors in rainfall measurements using a new type of gauge, Agricultural and Forest Meteorology, 98-99, 341–348, https://doi.org/10.1016/S0168-1923(99)00107-0, 1999.

Sevruk, B.: Point precipitation measurements: why are they not corrected?, in: Water for the future: Proceedings, edited by: Rodda, J. C., IAHS Pr. Inst. of Hydrology, Wallingford, 477–486, 1987.

Sevruk, B.: Methods of correction for systematic error in point precipitation measurement for operational use, Operational hydrology report, 21, WMO, Geneva, 91 pp., 1982.

Sevruk, B.: Correction for the wetting loss of a Hellmann precipitation gauge., Hydrological Sciences Bulletin, 549–559, 1974.

Sevruk, B. and Chvíla, B.: Error sources of precipitation measurements using electronic weight systems, Atmospheric Research, 77, 39–47, https://doi.org/10.1016/j.atmosres.2004.10.026, 2005.

Sevruk, B. and Hamon, W. R.: International Comparison of National Precipitation Gauges with a Reference Pit Gauge, WMO Instrument and Observing Methods Report, Geneva, No. 17, 1984.

Sevruk, B., Hertig, A. H., and Spiess, R.: Wind Field Deformation Above Precipitation Gage Orifices, in: IAHS-AGU Symposium on Atmospheric Deposition, edited by: Delleur, J. W. and Miller, J. M., 65–70, 1989.

Sevruk, B. and Nespor, V.: The Effect of Dimensions and Shape of Precipitation Gauges on the Wind-Induced Error, in: Global Precipitations and Climate Change, edited by: Desbois, M. and Désalmand, F., Springer, Berlin, Heidelberg, 231–246, https://doi.org/10.1007/978-3-642-79268-7_14, 1994.

Shedekar, V. S., King, K. W., Fausey, N. R., Soboyejo, A. B., Harmel, R. D., and Brown, L. C.: Assessment of measurement errors and dynamic calibration methods for three different tipping bucket rain gauges, Atmospheric Research, 178-179, 445–458, https://doi.org/10.1016/j.atmosres.2016.04.016, 2016.

Sugiura, K., Ohata, T., and Yang, D.: Catch Characteristics of Precipitation Gauges in High-Latitude Regions with High Winds, Journal of Hydrometeorology, 7, 984–994, https://doi.org/10.1175/JHM542.1, 2006.

Sugiura, K., Yang, D., and Ohata, T.: Systematic error aspects of gauge-measured solid precipitation in the Arctic, Barrow, Alaska, Geophys. Res. Lett., 30, https://doi.org/10.1029/2002GL015547, 2003.

Tapiador, F. J., Navarro, A., Levizzani, V., García-Ortega, E., Huffman, G. J., Kidd, C., Kucera, P. A., Kummerow, C. D.,
950   Masunaga, H., Petersen, W. A., Roca, R., Sánchez, J.-L., Tao, W.-K., and Turk, F. J.: Global precipitation measurements
          for validating climate models, Atmospheric Research, 197, 1–20, https://doi.org/10.1016/j.atmosres.2017.06.021, 2017.

Unold, G. von and Fank, J.: Modular Design of Field Lysimeters for Specific Application Needs, Water Air Soil Pollut:
          Focus, 8, 233–242, https://doi.org/10.1007/s11267-007-9172-4, 2008.

Vaughan, P. J. and Ayars, J. E.: Noise Reduction Methods for Weighing Lysimeters, J. Irrig. Drain Eng., 135, 235–240,
955   https://doi.org/10.1061/(ASCE)0733-9437(2009)135:2(235), 2009.

Vuerich, E., Monesi, C., Lanza, L., Stagi, L., and Lanzinger, E.: WMO Field Intercomparison of Rainfall Intensity Gauges,
          World Meteorological Organisation - Instruments and Observing Methods Rep. No. 99, WMO/TD No. 1504, 2009.

Watson, S., Smith, C. D., Lassi, M., and Misfeldt, J.: An Evaluation of the Effectiveness of the Double Alter Wind Shield for
          Increasing the Catch Efficiency of the Geonor T-200B Precipitation Gauge, CMOS Bulletin SCMO, 36, 168–175, 2008.

960   Wickham, H.: ggplot2: Elegant graphics for data analysis, Second edition, Use R!, Springer, Switzerland, 260 pp., 2016.

Winder, P. and Paulson, K. S.: The measurement of rain kinetic energy and rain intensity using an acoustic disdrometer,
          Meas. Sci. Technol., 23, 15801, https://doi.org/10.1088/0957-0233/23/1/015801, 2012.

WMO: Guide to Meteorological Instruments and Methods of Observation: Volume I - Measurement of Meteorological
          Variables, WMO, 8, World Meteorological Organization, Geneva, 1177 pp., 2018.

965   WMO: Guide to hydrological practices, 6th ed., World Meteorological Organization, Geneva, 2 pp., 2008.

Wolff, M. A., Isaksen, K., Petersen-Øverleir, A., Ødemark, K., Reitan, T., and Brækkan, R.: Derivation of a new continuous
          adjustment function for correcting wind-induced loss of solid precipitation: results of a Norwegian field study, Hydrol.
          Earth Syst. Sci., 19, 951–967, https://doi.org/10.5194/hess-19-951-2015, 2015.

Wong, K. and Nitu, R.: CIMO SURVEY ON NATIONNAL SUMMARIES OF METHODS AND INSTRUMENTS FOR
970   SOLID PRECIPITATION MEASUREMENT AT AUTOMATIC WEATHER STATIONS, INSTRUMENTS AND
          OBSERVING METHODS REPORT No. 102, WMO, Swizerland, 2010.

Xiao, H., Meissner, R., Seeger, J., Rupp, H., and Borg, H.: Effect of vegetation type and growth stage on dewfall,
          determined with high precision weighing lysimeters at a site in northern Germany, Journal of Hydrology, 377, 43–49,
          https://doi.org/10.1016/j.jhydrol.2009.08.006, 2009a.

975   Xiao, H., Meissner, R., Seeger, J., Rupp, H., and Borg, H.: Testing the precision of a weighable gravitation lysimeter, Z.
          Pflanzenernähr. Bodenk., 172, 194–200, https://doi.org/10.1002/jpln.200800084, 2009b.

Yang, D.: Double Fence Intercomparison Reference (DFIR) vs. Bush Gauge for "true" snowfall measurement, Journal of
          Hydrology, 509, 94–100, https://doi.org/10.1016/j.jhydrol.2013.08.052, 2014.

Yang, D., Goodison, B., Metcalfe, J., Louie, P., Elomaa, E., Hanson, C., Golubev, V., Gunther, T., Milkovic, J., and Lapin,
980   M.: Compatibility evaluation of national precipitation gage measurements, J. Geophys. Res., 106, 1481–1491,
          https://doi.org/10.1029/2000JD900612, 2001.

Yang, D., Kane, D. L., Hinzman, L. D., Goodison, B. E., Metcalfe, J. R., Louie, P. Y. T., Leavesley, G. H., Emerson, D. G.,
          and Hanson, C. L.: An evaluation of the Wyoming Gauge System for snowfall measurement, Water Resour. Res., 36,
          2665–2677, https://doi.org/10.1029/2000WR900158, 2000.

985   Yang, D., Goodison, B. E., Metcalfe, J. R., Louie, P., Leavesley, G., Emerson, D., Hanson, C. L., Golubev, V. S., Elomaa,
          E., Gunther, T., Pangburn, T., Kang, E., and Milkovic, J.: Quantification of precipitation measurement discontinuity
          induced by wind shields on national gauges, Water Resour. Res., 35, 491–508, https://doi.org/10.1029/1998WR900042,
          1999a.

Yang, D., Ishida, S., Goodison, B. E., and Gunther, T.: Bias correction of daily precipitation measurements for Greenland, J.
990   Geophys. Res., 104, 6171–6181, https://doi.org/10.1029/1998JD200110, 1999b.

Yang, D., Goodison, B. E., Ishida, S., and Benson, C. S.: Adjustment of daily precipitation data at 10 climate stations in Alaska: Application of World Meteorological Organization intercomparison results, Water Resour. Res., 34, 241–256, https://doi.org/10.1029/97WR02681, 1998.

Zacharias, S., Bogena, H., Samaniego, L., Mauder, M., Fuß, R., Pütz, T., Frenzel, M., Schwank, M., Baessler, C.,
995   Butterbach-Bahl, K., Bens, O., Borg, E., Brauer, A., Dietrich, P., Hajnsek, I., Helle, G., Kiese, R., Kunstmann, H., Klotz, S., Munch, J. C., Papen, H., Priesack, E., Schmid, H. P., Steinbrecher, R., Rosenbaum, U., Teutsch, G., and Vereecken, H.: A Network of Terrestrial Environmental Observatories in Germany, Vadose Zone Journal, 10, 955–973, https://doi.org/10.2136/vzj2010.0139, 2011.

Zhang, Q., Wang, S., Yue, P., and Wang, S.: Variation characteristics of non-rainfall water and its contribution to crop water
1000   requirements in China's summer monsoon transition zone, Journal of Hydrology, 578, 124039, https://doi.org/10.1016/j.jhydrol.2019.124039, 2019.